RNPS No. 2142
ISSN 2072-6287
Versión Digital

CENATAV
Centro de Aplicaciones de Tecnologías de Avanzada
MINISTERIO DE LA INDUSTRIA BÁSICA

REPORTE TÉCNICO
Reconocimiento de Patrones

SERIE AZUL

Iris Features Extraction Methods. Update 2013

Yasser Chacón-Cabrera,
José Luis Gil-Rodríguez, and
Eduardo Garea-Llano

RT_060 **febrero 2014**

7ma. No. 21812 e/218 y 222,
Rpto. Siboney, Playa;
La Habana.
Cuba. C.P. 12200
www.cenatav.co.cu

RNPS No. 2142
ISSN 2072-6287
Versión Digital

SERIE AZUL

REPORTE TÉCNICO
Reconocimiento de Patrones

CENATAV
Centro de Aplicaciones de Tecnologías de Avanzada
MINISTERIO DE LA INDUSTRIA BÁSICA

Iris Features Extraction Methods. Update 2013

**Yasser Chacón-Cabrera,
José Luis Gil-Rodríguez, and
Eduardo Garea-Llano**

RT_060 **febrero 2014**

7ma. No. 21812 e/218 y 222,
Rpto. Siboney, Playa;
La Habana.
Cuba. C.P. 12200
www.cenatav.co.cu

Table of Content

List of Figures

List of Tables

Iris Features Extraction Methods. Update 2013

Yasser Chacón-Cabrera, José Luis Gil-Rodríguez, and Eduardo Garea-Llano

Equipo de Investigaciones de Imágenes y Señales, Centro de Aplicaciones de Tecnología de Avanzada (CENATAV),
La Habana, Cuba
{ychacon,jlgil,egarea}@cenatav.co.cu

RT_060, Serie Azul, CENATAV
Aceptado: 12 de diciembre de 2013

Abstract. The human iris has proved to be a good and high-confidence biometric characteristic for the person verification and identification tasks due to its reliability, stability, uniqueness and hard to duplicate. One of the important tasks in iris recognition process is the feature extraction from the iris texture patterns. Looking the main publications of this subject can be said that feature extraction of iris texture is an open issue because: 1) there is not standard methods for feature extraction, therefore 2) have used different methods and viewpoints. This work presents an overview of iris features extraction methods, besides the characteristics of several methods are discussed. Also present a taxonomy of these techniques, discuss some experimental results and the conclusion of the works that were consulted, also analyze the challenges of the issue within the new trend of iris recognition.

Keywords: iris recognition, texture analysis, feature extraction.

Resumen. El iris humano ha demostrado ser un rasgo biométrico de alta confianza por a su estabilidad, fiabilidad, cualidad única, técnica no invasiva y difícil de duplicar. Una de las tareas más importantes en el proceso de reconocimiento del iris es la extracción de rasgos a partir de los patrones de textura del iris. Observando las principales publicaciones de esta temática se puede decir que la extracción de rasgos de la textura del iris es un tema aún no resuelto debido a: 1) la no existencia de un estándar para la extracción de rasgos, por lo que 2) se han utilizado diferentes técnicas y puntos de vista. Este trabajo presenta una panorámica de los métodos de extracción de rasgos en el iris. Se discuten las características de los principales enfoques. Se presenta también una taxonomía de estas técnicas, se discutirán algunos resultados experimentales y conclusiones de los trabajos examinados. Además se analizan los retos del tema dentro de las nuevas tendencias del reconocimiento biométrico del iris.

Palabras clave: reconocimiento de iris, análisis de textura, extracción de rasgos.

1. Introduction

In 1986 M. Alphonse Bertillon, a French anthropologist, proposed the use of iris patterns, particularly the color and shape, for the recognition persons[13]. In those remote times the discriminating iris features were extracted through the specialists observation, did not yet exist automatic methods. It was not until 1987 when the first patent[14] on the general concept of iris-based recognition appear and years later, in 1993, Daugman develop the most popular and commercial method[6] in the early history of iris biometrics. Since then, growing interest has been shown in iris recognition and in recent years has been significantly increased, it has also achieved great progress in terms of effectiveness and efficiency of the methods.

However, there is still much done to improvements performance and further the practical implementation of iris recognition systems under a variety of uncontrolled conditions. Recently iris recognition in terms of visible light has become the center of attention in this area.

The iris pattern compared to other biometric features has some advantages such as[15]:

- The iris begins to form in the third month of gestation and the structures creating its pattern are invariant.
- The forming of iris depends on the initial environment of embryo, so the iris texture patterns do not correlate with genetic determination.
- The left and right irises for a given person are different from each other.
- The inner organs of iris are protected by aqueous humor and cornea from the environment.
- The iris recognition is non-intrusive.
- It is almost impossible that irises are modified by surgical without risk.

One of the important tasks in iris recognition process is the feature extraction from the iris texture patterns. Looking at the different approaches to analyze the iris texture can say that has been the most popular area of research in iris biometrics[16].

The general concept of Biometric Feature Extraction Process [1] is defined as: the process applied to a biometric sample with the intent of isolating and out putting repeatable and distinctive numbers or labels which can be compared to those extracted from other biometric samples.

In the particular case of the iris biometrics the feature extraction objective is extract discriminative features from iris texture and stored in a more compact form so that it is more effective performing pattern matching in the following stage[17]. But, which are the most significant features and distinctive? what is the minimum amount needed? is there any way to automatically learn what features are best for the classifier[18]?. This question is not completely resolved today.

Is clear that the extracted features should meet at least the following requirements[7]:

- Significant: so that the iris image signature is an effective representation of the original iris image.
- Compact: so that the similarity measurement could be compute quickly.
- Fast: we have to process a large collection of images. Also we might have to extract features from query image on line as well.

In this work we make a critical analysis of current approaches involving this hot topic, both with their advantages and problems. Section 2 presents the main iris features extraction methods proposed and taxonomic classification of these. Section 3 discusses some experimental results, analysis and conclusions are found in the works consulted. Section 4 deals with the challenges iris feature extraction, and finally, the conclusions of the report.

1.1. Basic Steps in Iris Recognition

A typical iris recognition system consists of the following stages: iris image acquisition, iris segmentation, feature extraction, and pattern matching. Image acquisition has a great importance in iris recognition performance because the better the image quality, the more accurate result the system can achieve. After iris image is acquired, the next step is to locate the position of the iris and pupil. Several techniques have been proposed and most of them are based on image gradient and edge detection. After iris has been located, features of the iris texture scan are extracted. Which features should be extracted and how

[1] Biometrics Identity Management Agency, Biometrics Glossary, April 2012 Version.6

to extract them is also important issue in iris recognition? Good features give high inter-class variation and low within-class variation, which is desired in common biometric recognition system. Finally, one should be able to compare features from different irises and obtain a score of similarity which tells how similar these two irises are (or a score of distance, which tells how much different they are). Decision of classifying test image as authentic or imposter is made by comparing the similarity score with a given threshold[19].

2. Iris Features Extraction Methods

This section is the main core of this work, in will be discussed the principal methods of the iris features extraction update to nowadays. The features extraction is based on algorithms that analyze the segmented and normalized iris image in order to extract the distinctive features from the iris texture pattern, that will be used in the process of people recognition.

The iris has a particularly interesting structure and provides abundant texture information. So, it is desirable to explore representation methods which can describe global and local information in an iris[20]. In this sense, several strategies have been employed with analysis outlines that make use of: a) signal processing methods, in spatial domain and also in frequencies domain of the iris data. This group of methods makes use of digital filtering technique to describe the iris texture, b) statistical processing methods, looking for to stand out the existence of spatial relationships between different iris texture regions, c) the employment of combined techniques, to describe the texture as better as possible and also in exhaustive way, taking advantage of the description power using several analysis sources.

At the following session, we present a taxonomy, see Fig.1., of the most used and recognized feature extraction methods to describe and represent numerically the iris texture.

2.1. A Taxonomy of Methods

The texture's features obtained from the second-order[21] statistics methods like co-ocurrence, Local Binary Pattern(LBP) have been introduced to exploit the spatial dependencies that characterize the image texture, but basically this kind of texture descriptor only give information about the events that take place in a single scale. When the texture patterns are present with sizes of various scales, and in different angular directions, then these methods are not the most suitable. However, the Independent Component Analysis(ICA) method is a statistical technique that aims is to reveal interesting hidden relationships and factors within sets of original variables. Therefore, the ICA method is possible apply it to a set of texture features extracted from the iris using any texture descriptor method. The result is a new features set reveled with new properties which are useful in order to interpret the iris texture[22].

The signal processing technique possesses the main powerful methods for texture feature extraction. They have as theoretical principles the modification of the spectral composition of image using mathematical operator on the spatial domain, or using some transform, like Fourier, Gabor or Wavelets transform, to extract texture features at the frequency domain. These kinds of technique are known as spectral techniques. It is based on digital filtering properties and facilitates the noise removal on the images acquired during the capture process. This process of image filtering modifies the spectral composition, low frequencies (or high frequencies) in the image. The digital filtering using Gabor filters and Wavelets filters describe the iris texture in the context of several scales. This kind of texture descriptors uses banks of filters to quantify the energy of the texture in different scales using several frequencies and angular directions in the image.

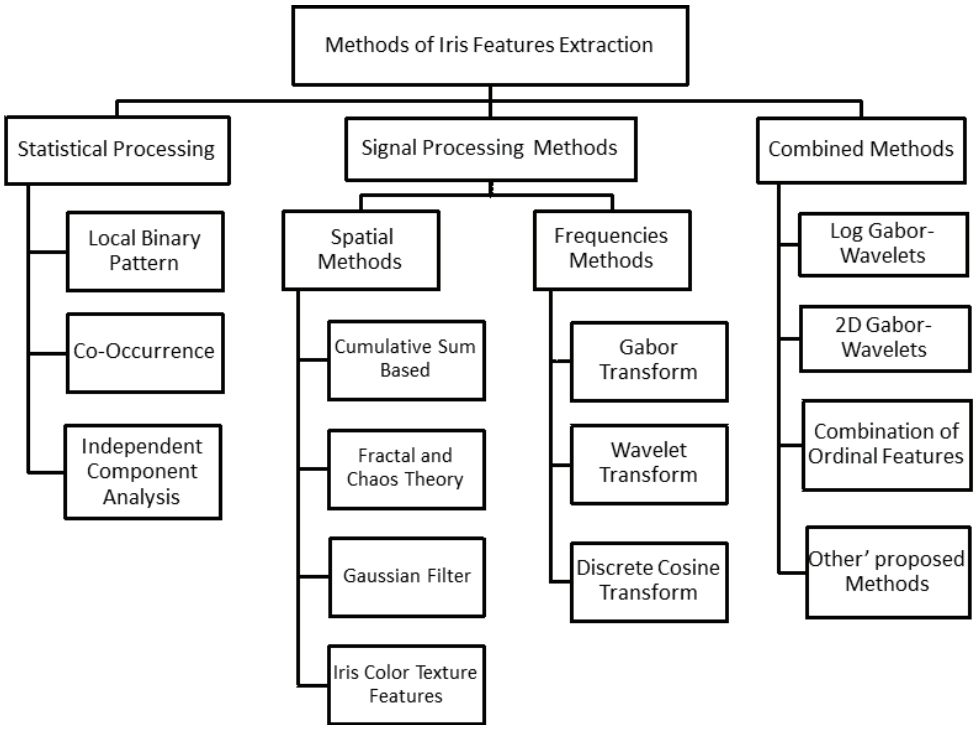

Fig. 1. Proposal Taxonomy of the Iris features extraction methods more widely used nowadays.

The combined methods make use of the feature fusion obtained from several individual methods, and that synergy of iris features provides greater ability to describe the iris texture, and thus provides high capacity for individual recognition. The next sections provide data in detail on each of the methods depicted in taxonomy presented.

2.2. Statistical Processing

2.2.1. Local Binary Pattern

LBP is an efficient method used for feature extraction and texture classification, it was first introduced by Ojala et al.[23] in 1996. The LBP operator was introduced as a complementary measure for local image contrast, and it was developed as a gray scale invariant pattern measure adding complementary information to the "amount" of texture in images. LBP is ideally suited for applications requiring fast feature extraction and texture classification.

Sun, Tan et al.[24] used LBP for iris recognition. Their method divided the upper region of the normalized iris image into $2\times16=32$ blocks, and each block has the size 32 by 32. For each block in the normalized iris image, an eight-neighborhood uniform LBP histogram with radius 2 (59 bins) may be obtained. In their labeled graph representation of iris pattern, each manually divided image block is regarded as a graph node, associated with the attributes of the local region's LBP histogram. The spatial layout of these image blocks is used to model the structural relations among the nodes. Finally, a graph with 32 nodes is constructed as the template of each iris image. This template is use for matching.

Tian, Qu et al.[25] used LBP features extraction in two rectangular neighborhoods (size 3×3 and 5×5). Then selected most stable and effectiveness features by comparing intra images of the same iris. In the experiments, the authors only compared LBP with feature selection vs LBP without feature selection.

Rashad, Shams et al.[1] proposed an algorithm for iris recognition and classification using a system based on LBP and on histogram properties as a statistical approach for feature extraction, and Combined Learning Vector Quantization Classifier (LVQ) as Neural Network approach for classification, see Fig.2 general structure of proposed method. The authors first extract LBP features of small regions in which they divided the normalized iris image, then creating a LBP histograms for each region, finally connecting the histograms obtained in a single histogram.

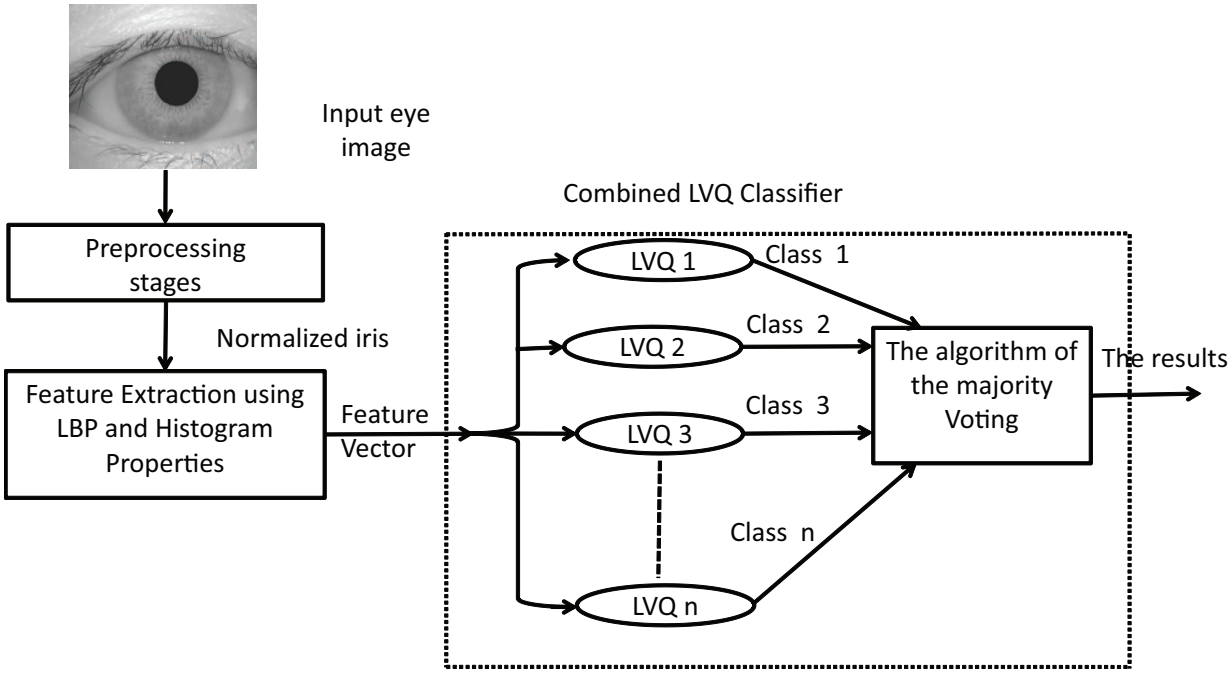

Fig. 2. General structure of proposed method by Rashad, Shams et al.[1].

Marsico, Nappi et al.[26] deal with an approach to iris matching based on the combination of local features: LBP and discriminable textons (BLOBs). They divided the iris image into horizontal (or vertical) bands. For each band, the histogram of LBP values is computed. The result code C [2] will be stored as a sequence of histograms plus the related noise mask $M : C = (H_1, H_2, ..., H_{bands}, M)$. Such features can be considered BLOBs: a group of image pixels which form a structure which can be darker or lighter than the surrounding region. The extraction of the BLOBs from an iris image is obtained through different LoG (Laplacian of Gaussian) filter banks, this technique they call BLOB. The final method for coding and matching LBP-BLOB is define as Eq.1:

- Coding of the pair (I, M) is $c = C_{LBP}, C_{BLOB}$.
- Matching between codings c_1 and c_2 is given by:

$$\delta(C_1, C_2) = \frac{\delta_{LBP}(C_{1,LBP}, C_{2,LBP})}{2} + \frac{\delta_{BLOB}(C_{1,BLOB}, C_{2,BLOB})}{2} . \quad (1)$$

This work obtained sixth place in NICE.II iris biometrics competition[3]

[2] LBP code C is computed as the difference of the average pixels with threshold equal 1 and average pixels with threshold equal 0

[3] http://nice2.di.ubi.pt/

2.2.2. Co-Occurrence

Li, Liu et al.[27] presented a weighted co-occurrence phase histogram (WCPH) for representing the local characteristics of texture pattern. The method proposed a weighting function that enables a phase angle to make contributions to several adjacent bins; the co-occurrence histogram considers the information of both, the phase angle and spatial layout; and they introduce a Bhattacharyya distance measure for evaluating the goodness of match between two WCPHs. Also WCPH is distinctive and insensitive to illumination changes and noise.

Let ς be the set of all points in a gray level image S, and denote by $S(z)$ the pixel value at the spatial point $z = (x,y)$. Using an edge detector, for example, the *Sobel* operator, they can compute the gradients of the image S. Let g_z and θ_z be the gradient magnitude and phase angle at z, respectively. Suppose the interval $[0, 2\pi]$ is uniformly divided into m bins. The rotationally invariant co-occurrence histogram $\widetilde{p}_{\varsigma,d} = \{\widetilde{p}_{\varsigma,d}(u,v)\}_{u,v=1,\ldots,m})$ considers all pairs of pixels that are at fixed distance d, where $\widetilde{p}_{\varsigma,d}(u,v)$ is defined as Eq.2:

$$\widetilde{p}_{\varsigma,d}(u,v) = \frac{1}{\widetilde{C}_{\varsigma,d}} \sum_{Z \in \varsigma} \sum_{\|Z-Z'\|=d} \delta(u,\theta_z)\delta(v,\theta_{z'}) \;, \tag{2}$$

where $\|.\|$ denotes the L_2-norm, $\delta(u,\theta_z)$ is the Kronecker function that equals 1 if θ_z falls into bin u and equals 0 otherwise, and $\widetilde{C}_{\varsigma,d}$ denotes the number of point pairs. The co-occurrence histogram defines the joint probability of pairs of two points that are at distanced of each other. This method ranked the fifth place in NICE.II Competition.

2.2.3. Independent Component Analysis

ICA is a statistical and computational technique for revealing hidden factors that underlie sets of random variables, measurements, or signals[28].

ICA defines a generative model for the observed multivariate data, which is typically given as a large database of samples. In the model, the data variables are assumed to be linear mixtures of some unknown latent variables, and the mixing system is also unknown. The latent variables are assumed non-Gaussian and mutually independent and they are called the independent components of the observed data. These independent components, also called sources or factors, can be found by ICA[28].

The iris recognition system developed by Ya-Ping, Si-Wei et al.[29] adopts ICA to extract iris texture features. The authors represents iris pattern with ICA coefficients, then determines the center of each class by competitive learning mechanism and finally recognizes the pattern based on Euclidean distances. The basis function used is kurtosis denoted by Eq.3:

$$kurt(y) = E\{y^4\} - 3(E\{y^2\})^2 \;. \tag{3}$$

To improve the computational cost, the authors propose, work with patches of images of size N×N and estimate the coefficients in ICA image patches.

Dorairaj, Schmid et al.[2] analyzed the performance of two encoding strategies Principal Component Analysis (PCA) and ICA that are capable of capturing both global and local features when applied to an iris image, see Fig.3. The authors also consider the possible rotation of the normalized iris image due to poor image alignment and not divide the iris images in patches.

In Chowhan and Shinde[30], the authors, used PCA and ICA. PCA has been used as a preprocessing step that reduces dimensions for obtaining ICA components for iris. The experimental results demonstrate that the ICA algorithms are very effective when using very good quality iris images with a small size. However, in the case of noisy and deformable iris images with large block size, the performances of

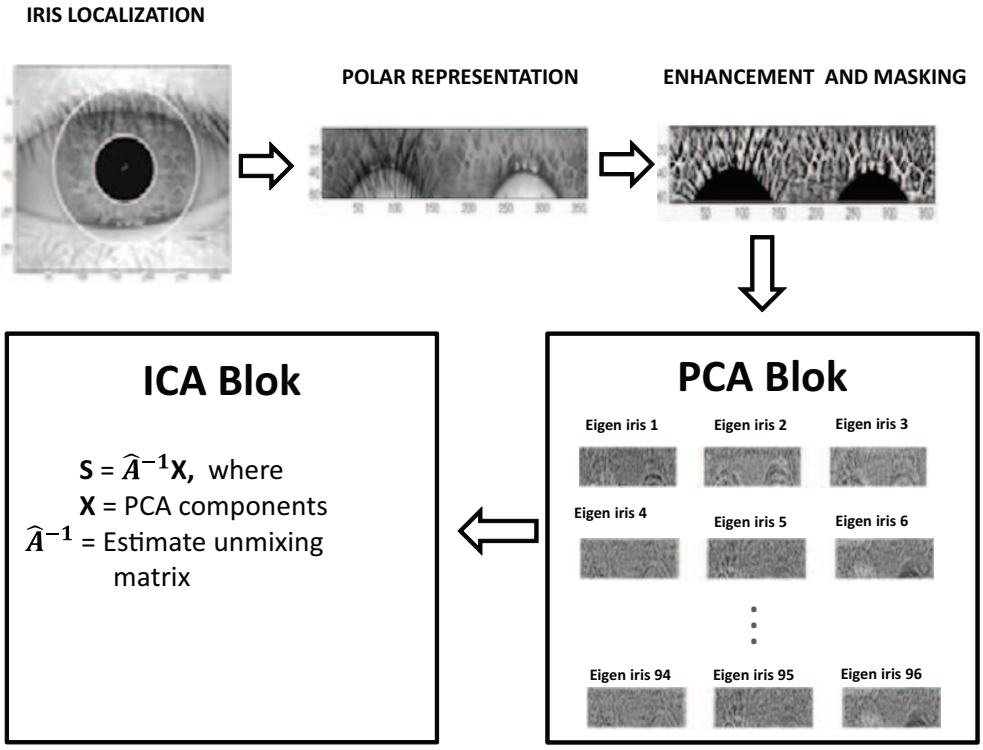

Fig. 3. Block-diagram of the system implementing PCA/ICA encoding techniques for iris proposed by Dorairaj, Schmid et al.[2].

the Fast-ICA and ICA by relative Newton method get marginally better when compared against JADE algorithm. However, in general, the obtained results allow them to conclude that ICA could perform well for such application, but it is sensitive to illumination and noise degradations caused by the eyelids and eyelashes. This is a limitation of ICA based-methods.

In Bouraoui, Chitroub et al.[31], restudied the application of ICA for a possible improvement of iris recognition. They implemented an experiment with JADE algorithm, ICA by relative Newton method and Fast-ICA algorithm. The best results are obtained with ICA by relative Newton method when image patch size is 8×8 pixels and JADE algorithm when image patch size is 16×16 pixels for CASIA-Iris V3-Interval database. However, the results obtained with the Fast-ICA algorithm are the worse with block of 16×16 pixels for the CASIA-IrisV3-Interval database. However, the CASIA-IrisV3-Lamp database gives better results than those obtained by JADE for blocks of 16×16 pixels. Furthermore, JADE algorithm yields good results for blocks 16×16 pixels when using CASIA-IrisV3-Lamp database.

2.3. Spatial Methods

2.3.1. Cumulative Sum-Based

The method proposed by Jong-Gook[32] used a cumulative-sum-based[4] change analysis to extract features from iris images following this step:

[4] Change-Point Analysis: A Powerful New Tool For Detecting Changes URL:http://www.variation.com/cpa/tech/changepoint.html

1. Divide normalized iris image into basic cell regions for calculating cumulative sums. One cell region has 3(row)×10(col) pixels size. An average grey value is used as a representative value of a basic cell region for calculation.
2. Basic cell regions are grouped horizontally and vertically (Five basic cell regions are grouped together because experimental results show that much better performance is achieved when a group consists of five cells).
3. Calculate cumulative sums over each group as in (2).
4. Generate iris feature codes.

Cumulative sums are calculated as follows. Suppose that $X_1, X_2, ...,$ and X_5 are five representative values of each cell region within the first group located on the left top corner.

- Calculate the average $\overline{X} = (X_1 + X_2 + ... + X_5)/5$
- Calculate cumulative sum from $0 : S_0 = 0$.
- Calculate the other cumulative sums by adding the difference between the current value and the average to the previous sum Eq.4:

$$S_i = S_{i-1} + (X_i - \overline{X}) \, for i = 1, 2, ..., 5 \; . \tag{4}$$

Cumulative sums are calculated by addition and subtraction, so the cumulative-sums-based feature extraction method creates a lower processing burden than other methods. After calculation, Iris codes are generated for each cell using the following algorithm:

Iris_code_generation {
for (2 times loop){ \\ *for horizontal and vertical directions*
MAX = max(S1,S2,???,S5); MIN = min(S1,S2,???,S5);
if Si located between MAX and MIN index
if (Si on upward slope) set cell's iris_code to 1
if (Si on downward slope) set cell's iris_code to 2 else
set cell's iris_code to 0
} }

The algorithm proposed by Rathgeb and Uhl[33] is similar to the approach in Jong-Gook. First the authors discarded the top and bottom of the iris because are often hidden by eyelashes or eyelids. Then tracing light and dark intensity variations of gray scale values in horizontal stripes of distinct height, pixel-paths are extracted. For a height of 3 pixels each position within pixel-paths is encoded using 2 bits. For a total number of 21 pixels the resulting iris-code consists of 10.752 bits[34].

2.3.2. Fractal and Chaos Theory

Ebrahimzadeh, Jampour et al.[35] proposed the technique iris identification based-Fractal and Chaos Game Theory (Iris-IFCGT). This technique has some fractal properties like stability against zoom, removing part of the iris image, no sensitivity on rotation and so on as well as desirable speed which helps preventing time consuming process of pattern Recognition.

fractal objects have three important properties self-similarity, iterative formation and fractional dimension. It means that fractal body parts are similar to body and are produced by a repetitive process. In Chaos Game Theory new fractal can be produced by random walk process and polygons of a fractal. One important point in this technique is that during the Chaos Game mechanism in producing a new fractal some parameters can be extracted, so that they are useful for identification. The authors used rectangle

in the mechanism of Chaos Game Theory, repeat for 50,000 times, and extract some parameters that are unique for each iris.

The authors believe that the method is robust to rotation and low computational cost. In this work there is not comparison with existing methods.

2.3.3. Gaussian Filter

Laplacian of Gaussian

For the process of feature extraction, Wildes[36], performed isotropic band-pass decomposition using Laplacian of Gaussian (LoG) filters defined as Eq.18:

$$G = -\frac{1}{\pi\sigma^4}(1-\frac{\rho^2}{2\sigma^2})e^{-\rho^2/2\sigma^2}\ , \tag{5}$$

where, σ is the standard deviation of the Gaussian and ρ is de radial distance of a point from the filter's center, respectively. The result of decomposition is a Laplacian pyramid of four levels.

The essence of feature extraction in Wilde's algorithm[36] was used to capture the range of spatial structures using two-dimensional band-pass decomposition, where every level encompassed two steps[37]:

1. Low pass filtering of the iris and down-sampling by a factor 2 on the horizontal and vertical directions.
2. Starting from the smallest image, it is expanded by a factor 2 (up-sampling with linear interpolation) and subtracted from the one which is one level below.

With this expansion, four band-pass iris images were acquired and used as the biometric template. Matching was performed using a shift, scale and rotate methodology which given a pixel at the template image seeks to establish a match with any pixel of the input image[37].

Lu and Lu[38] designed a bank of LoG filters with different scales (they chosen four scales with $t = 1,4,9,16$). They compared each sample point of filtered images to its eight neighbors in the current scale and nine neighbors in the scale above and below. It is selected only if it is larger than all of these neighbors.

Chou, Shih et al.[39] used two filters derived of LoG. The filters are then convolved with images to get filtered images. If the filtered images have intensity greater than 0 it is likely that there is a ridge at that location[37]. The method work well when the iris image is acquired angles off-axis.

Ordinal Measures

Ordinal Measures (OMs)[5] come from a simple and straightforward concept that we often use. For example, we can easily rank or order the heights or weights of two persons, but it is hard to tell their precise differences. This kind of qualitative measurement, which is related to the relative ordering of several quantities, is defined as OMs[40].

The idea of OMs for iris recognition, proposed by Sun and Tan [40], comes from their two previous works: local ordinal measures and nonlocal ordinal measures.

- In Local Ordinal Measure[41], the richness of inter-region sharp intensity variations provides a good source of OMs for class model construction. They defined robust direction estimation (RDE), to estimate the local dominant direction of gradient, and to encode local image relationships.

[5] It was decided include OMs in this session due to the particular filter used by the authors for your implementation.

- In Non-local Comparisons[42], they analyzed that existing iris recognition methods only used the local relative relationships, ignoring the rich ordinal information between the long-distance regions. Long-distance comparisons are more tolerant to common image degradations than purely local ones. They defined "Dissociated Multi-Pole", extensions of Balas and Sinha[43] work, to encode the non-local image relationships.

Sun and Tan[40] defined multilobe differential filters (MLDFs) to compute OMs with flexible intralobe and interlobe parameters such as location, scale, orientation, and distance. Mathematically, the MLDFs are given as follows when Gaussian kernel is employed as the basic lobe Eq.6:

$$MLDF = C_p \sum_{i=1}^{N_p} \frac{1}{\sqrt{2\pi\delta_{pi}}} exp[\frac{-(X-\mu_{pi})^2}{2\delta_{pi}^2}] - C_n \sum_{j=1}^{N_n} \frac{1}{\sqrt{2\pi\delta_{nj}}} exp[\frac{-(X-\mu_{nj})^2}{2\delta_{nj}^2}] \,, \tag{6}$$

where the variables μ and δ denote the central position and the scale of a 2D Gaussian filter, respectively; N_p the number of positive lobes; and N_n the number of negative lobes. Constant coefficients C_p and C_n are used to ensure zero sum of the MLDF, i. e. , $CpNp = CnNn$. The most compelling feature of MLDF compared with traditional differential filters is that it decouples the settings of intralobe (scale) and interlobe (distance) parameters. So, multilobe differential filters can be used to encode OMs of both connected and dissociated image regions[40].

The procedure of iris feature using MLDF is as follows: An MLDF operator slides across the whole normalized iris image and each ordinal comparison is encoded as one bit, i. e. , 1 or 0 according to the sign of the filtering result. All of the binary iris codes constitute a composite feature of the input iris image, namely, ordinal code (OC)[40].

A large pool of regional ordinal features is therefore generated. Definitely, this feature pool must contain much redundant information because of the redundancy between different ordinal filters as well as that between different subregions. To attack this poblem, Zhaofeng, Zhenan et al. [44], developed a Similarity Oriented Boosting (SOBoost) algorithm to train an efficient and stable classifier with a small set of features. Wang, Sun et al. [45] proposed algorithm based on linear programming, which can learn a compact and effective ordinal feature set for iris recognition an improve the previous works.

2.3.4. Iris Color Texture Features

Zhang, Sun et al.[3] introduced a novel iris color representation method named as iris color Texton, wich combines a pixel value in RGB, HIS and $\iota\alpha\beta$[46] color spaces as color feature and represents iris images by Texton voting method. The $\iota\alpha\beta$ color space is less used, one important property of this color space is that it can minimize the correlation between channels.

They combine values of a pixel in the RGB, HIS and $\iota\alpha\beta$ color spaces in series as color feature (9-D vector,$[r, g, b, h, s, \iota, \alpha, \beta]$ these values are normalized into $[0, 1]$). They divide a normalized image into three parts along vertical direction and extract color features from each part respectively. Then connect these feature to form final feature vector. First, several clustering centers are learned by K-means from each iris image as Major colors, which constitute the training feature pool. Last, a simple vocabulary optimization is done: abandoning Textons near maximum value corresponding to specular spots; abandoning Textons near to zero corresponding to shadow see Fig.4.

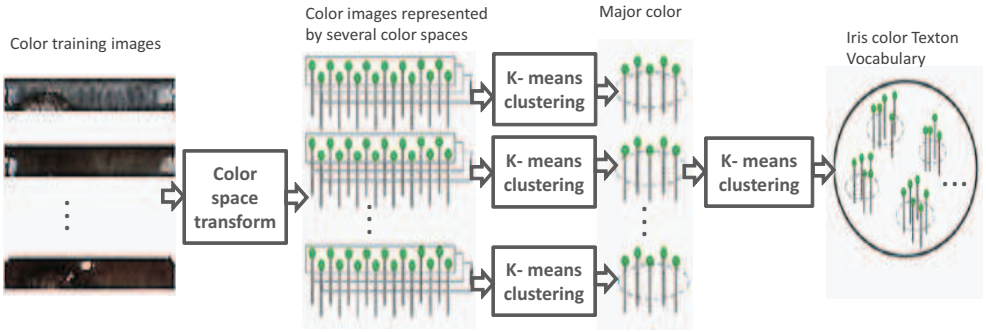

Fig. 4. Illustration of the iris color Texton vocabulary learning proposed by Zhang, Sun et al.[3].

2.4. Frequencies Methods

2.4.1. Gabor Filter

The Gabor filter was originally introduced by Dennis Gabor[47]. Gabor filters are bandpass filters which are used in image processing for feature extraction and texture analysis.

Gabor filters are able to provide optimum conjoint representation of a signal in space and spatial frequency. A Gabor filter is constructed by modulating a sine/cosine wave with a Gaussian. This is able to provide the optimum conjoint localization in both space and frequency, since a sine wave is perfectly localized in frequency, but not localized in space. Modulation of the sine with a Gaussian provides localization in space, though with loss of localization in frequency. Decomposition of a signal is accomplished using a quadrature pair of Gabor filters, with a real part specified by a cosine modulated by a Gaussian, and an imaginary part specified by a sine modulated by a Gaussian. The real and imaginary filters are also known as the even symmetric and odd symmetric components respectively.

The center frequency of the filter is specified by the frequency of the sine/cosine wave, and the bandwidth of the filter is specified by the width of the Gaussian[48].

2D Gabor Filter

A two-dimensional (2D) even Gabor filter can be represented by the following equation Eq.7 in the spatial domain:

$$\begin{aligned} G(x,y,\theta,f) &= exp\{-\frac{1}{2}[\frac{x'^2}{\sigma_{x'}^2}+\frac{y'^2}{\sigma_{y'}^2}]\}\cos(2\pi f x') \ , \\ x' &= x\cos\theta + y\sin\theta \quad , \\ y' &= y\cos\theta - x\sin\theta \ , \end{aligned} \tag{7}$$

where f is the frequency of the sinusoidal plane wave along angular the direction θ from the x- axis, $\sigma_{x'}$ and $\sigma_{y'}$ are the spatial constants of the Gaussian envelope along x' and y' axes respectively.

Daugman used a 2D version of Gabor filters[6] in order to encode iris pattern data. A 2D Gabor filter over the an image domain (x,y) is represented by Eq.8:

$$G(x,y) = e^{-\pi[(x-x_0)^2/\alpha^2+(y-y_0)^2]/\beta^2} e^{-2\pi i[\mu_0(x-x_0)+\upsilon_0(y-y_0)]} \ , \tag{8}$$

where (x_0, y_0) specify position in the image, (α, β) specify the width and length, and (μ_0, υ_0) specify modulation (this parameters allow the filter to be tuned to particular directions of pace and frequency modulation), which has spatial frequency $w_0 = \sqrt{\mu_0^2 + \upsilon_0^2}$ and direction $\theta_0 = \arctan(\frac{\upsilon_0}{\mu_0})$.

Yu, Zhang et al.[49] used multi-channel 2-D Gabor filters to get texture information in various directions and different scales. Each 2-D Gabor filter has an even-symmetrical real part and an odd-symmetrical imaginary part. They set four different values for $\theta : 0^0, 45^0, 90^0,$ and 135^0. In order to extract texture information in different scales, the wavelength is set to four discrete values: $4, 8, 16, 32$, so that there are $4 \times 4 = 16$ channels, 16×2 (even and odd)$= 32$ filters. In every filtered sub-image, they extract the points that represent the local texture most effectively in each channel. The barycenter of these points in each channel is called the key point and a group of key points are obtained. Then, the distance between the center of key points of each sub-image and every key point is called relative distance, which is regarded as the iris feature vector[50].

Qiu, Sun et al.[51] learned a small finite vocabulary of micro-structures that they called Iris-Textons, to represent visual primitives of iris images. To get the Iris-Textons the authors apply 2D Gabor filter (40 even) as filtering. Then they used Iris-Texton histograms to capture the difference between iris textures. Finally, all images are classified into two ethnic categories, Asian and non-Asian, through a trained Support Vector Machine(SVM).

Al-Qunaieer[52] investigated the use of colors in the process of iris identification. He derived 2D Gabor filter to the Quaternion Gabor filter Eq.9 by multiplying the unit quaternion μ with the real part of the filter as:

$$G(x,y) = \mu \frac{1}{2\pi\sigma_x\sigma_y} exp\{-\frac{1}{2}[\frac{x^2}{\sigma_x^2} + \frac{y^2}{\sigma_y^2}]\} \cos\{2\pi(ux + uy)\} \ . \tag{9}$$

The Gabor filter can be defined as a pure quaternion where its color component and pointing to a particular direction in the 3D color space. A unit quaternion μ , pointing to an interesting direction in the 3D color space, is multiplied with the previously defined Gabor filter in order to get the Quaternion Gabor Filter. The experiments show that the Quaternions can used successfully to represent the color image of iris.

In Wang et al.[53] the authors extract global and local texture information based on 2D Gabor filters[54] at different orientations. The filters is applied in whole iris image normalized (global) and is applied in overlapping patches M×N (local) in which was divided the normalized iris. They used Adaboost to select and combine the most discriminative features from feature set. This method obtained the second place in NICE.II.

Log-Gabor Filter

Log-Gabor filters were proposed by Field in 1987[55]. The 2D Log-Gabor filters Eq.10 are constructed in the polar coordinate system of frequency domain. They only can be numerically constructed in the spatial domain via the inverse Fourier transform:

$$G(\omega, \theta) = exp\{\frac{-\log(\frac{\omega}{\omega_0})}{2\log(\frac{k}{\omega_0})}\} exp\{\frac{-(\theta - \theta_0)^2}{2T(\Delta\theta)^2}\} \ , \tag{10}$$

where ω_0 represents the center frequency of the filter; k determines the bandwidth of the filter in the radial direction; θ_0 represents the orientation angle of the filter; T is a scaling factor and $\Delta\theta$ the orientation spacing between the filters.

As Eq.10 shows, Log-Gabor filters have Gaussian transfer functions when viewed on the logarithmic linear frequency scale. Compared with Gabor filters, Log-Gabor filters have two important characteristics. Firstly, Log-Gabor filters, by definition, always have no Direct Component(DC). Secondly, the transfer function of the Log-Gabor filters has an extended tail at the high frequency end[55].

One of advantages of Log-Gabor filters is that they are strictly bandpass filters. So no DC components will pass the filters. Therefore the background brightness will not affect the extraction of the pure phase information of iris texture[56].

Peng, Li et al.[56] changed the frequency expression of 2D Log-Gabor filters Eq.11 and construct it in the Cartesian coordinate system of frequency domain:

$$G(u,v) = exp\{\frac{-\log(\frac{u_1}{u_0})^2}{2\log(\frac{k}{u_0})}\}exp\{\frac{-v_1^2}{2\sigma_v^2}\}\ , \tag{11}$$

where $u_1 = u\cos(\theta) + v\sin(\theta), v_1 = -u\sin(\theta) + v\cos(\theta), \theta$ is the orientation of the 2D Log-Gabor filter, u_0 is the center frequency, k determines the bandwidth of the filter in the v_1 direction, and σ_v determines the bandwidth of the filter in the direction v_1.

Seif, Zewail et al.[57] used Bank of Log-Gabor filters at five different scales and four different orientations. The filters parameters are chosen to get even coverage of the spectrum. They calculated the average absolute deviation of gray values in the response of each filter and generated feature vector of length 320 entries.

Ng,Tay et al.[4] used 1D Log Gabor filter to extract the frequency information which represents the iris textures. They divided the normalized iris image in three zone $(Z_1, Z_2$ and $Z_3)$, see Fig.5. It is observed that the inner zone Z_1 contains the finest iris texture and extracted using Log Gabor filter with high center frequency ω_0. The middle zone Z_2 with larger block of texture is processed using filter with a lower center frequency. A coarsest filter with lowest center frequency is used to capture the flattest texture in the outer zone Z_3.

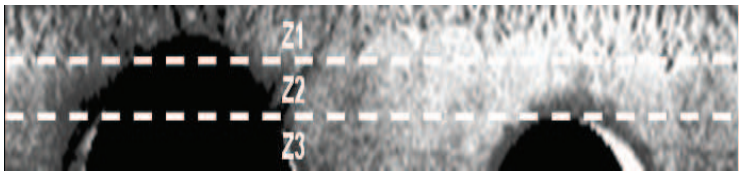

Fig. 5. The three zone in which the normalized iris image is divided proposed by Ng,Tay et al.[4].

Farouk and Elhadi[58] used 1D log-Gabor filter to extract real valued template for the normalized iris. Each row of the iris image, in the log-polar coordinates, is first transformed to the frequency domain using Fast Fourier Transform (FFT). This frequency domain row signal is then filtered with the 1D log-Gabor filter (i.e. multiplied with the 1D log-Gabor filter in the frequency domain). The filtered row signal is transferred back to the spatial domain via Inverse Fast Fourier Transform (IFFT). The spatial domain signal is then transferred to a filtered image in the spatial domain, and hence the biometric code (template) is obtained from the filtered image.

In Bastos, Tsang et al.[59], its presents an analysis of the parameters used to construct 2D log-Gabor filters to encode iris patterns. They encoded the iris patterns extracting only phase information, projecting the filtered phasor over the complex plane formed by the filter. In this process two bits per projection are acquired, resulting in a template with 9600 bits $(240 \times 20 \times 2)$. An equal number of bits are assigned to the noise mask, which mark areas such as eyelids, eyelashes, occlusions and reflections are detected at segmentation stage.

Other Gabor Filter

Jeong, Park et al.[60] proposed the Adaptive Gabor Filter Eq.11 that can be defined as follows:

$$G(x) = A.e^{-\pi[\frac{(x-x_0)^2}{\sigma^2}]}(\cos(2\pi[\mu_0(x-x_0)])), \Sigma_{x=-N}^{N} G(x) = 0(\because DC = 0) \ , \tag{12}$$

where A represents the amplitude of the Gabor filter $G(x)$, and σ and μ_0 are the kernel size and the frequency of Gabor filter, respectively. x_0 is the displacement amount of the Gabor filter. $2N$ is the Gabor filter coefficient. To make iris code generation is not affected by the image brightness of iris texture, they set the DC component to be 0).

Another algorithm Ma, Tan et al.[61] and Li, Yunhong et al.[62](shorter version of this method) is based on a bank of spatial filters. They define new spatial filters to capture local details of the iris. The difference between Gabor filter and the defined filter lies in the modulating sinusoidal function. The former is modulated by an oriented sinusoidal function, whereas the latter by a circularly symmetric sinusoidal function. Their kernels are given as follows Eq.13 :

$$\begin{aligned} G(x,y,f) &= \frac{1}{2\pi\delta_x\delta_y} exp\left[-\frac{1}{2}[\frac{x^2}{\delta_x^2}+\frac{y^2}{\delta_y^2}]\right] M_j(x,y,f); j = 1,2. \\ M_1(x,y,f) &= \cos[2\pi f(\sqrt{x^2+y^2})], \\ M_2(x,y,f) &= \cos[2\pi f(x\cos\theta + y\sin\theta)] \ , \end{aligned} \tag{13}$$

where $M_i(x,y,f)$ denotes the modulating function; M_1 and M_2 are the modulating function of the defined filter and Gabor filter, respectively; f is the frequency of the sinusoidal function; δ_x and δ_y are the space constants of the Gaussian envelope along the x and y axis, respectively; and θ denotes the orientation of Gabor filter.

2.4.2. Wavelet Transform

The first wavelet transform was the Haar wavelet, proposed about 1910. But the concept of wavelet was not popular until 1981 with the proposal of Jean Morlet. After that, the development of wavelet became flourishing. In the 1980s, there are lots of studies about wavelet, such as Daubechiess systematical method to constructs the compact support orthogonal wavelet, and Stephanen Mallat and Meyersmulti-resolution concept. However, the complexity of wavelet was still too complex for computation until 1989 when Mallat proposed the fast wavelet transform[63].

The fundamental idea behind wavelets is to analyze the signal at different scales or resolutions. Wavelets are a class of functions used to localize a given signal in both space and scaling domains[64]. A family of wavelets can be constructed from a mother wavelet. Wavelets mean small waves that segment data into different frequency components and transfer each matched component with different resolution to its scale. The main idea of wavelet analysis is to see both coarse and detailed data without heavy computational cost. The goal of most modern wavelet researches is to create a set of basic functions and transform them in order to give information[64].

Most standard wavelets, Eq.14, are based on one wavelet function, $\Psi(x)$, which has some special properties. The wavelet function have oscillation property, mathematically expressed by an integration to zero given by[65]:

$$\int_{-\infty}^{+\infty} \Psi(x)\, dx \equiv 0 \ . \tag{14}$$

Zhu, Tan et al.[66] described an algorithm which uses mean values and standard deviations of multiple 2D-wavelet subbands as features. A pyramidal wavelet subdivision (using the standard D4 wavelet) is performed on iris textures, which are obtained from a polar mapping of the region between the pupil circle and outer iris circle, as was described by Daugman. The features of the resulting subbands are extracted by computing mean value and standard deviation for each subband. In this way from each iris picture a feature vector is obtained containing a number of outing point values, one mean value and one standard deviation for each subband.

In the proposal of Ma, Tan et al.[67], the main idea is extract sharp variations of intensity signals. The normalized iris texture is divided into stripes to obtain 10 one-dimensional signals, each one averaged from the pixels of 5 adjacent rows (only the upper 512×50 rows are analyzed). Subsequently, a 1-D wavelet transform is applied to each of the ten 1-D intensity signals. Detected minima and maxima from two specific subbands serve as features where sequences of 1s and 0s are assigned to the iris-code until new maxima or minima are found. This whole process is applied to two subbands extracting a total number of $2 \times 512 \times 10 = 10{,}240$ bits[34].

Xiaofu and Pengfei[68] presented an iris feature extraction method by using two dimensional Complex Wavelet Transform (2D-CWT). The proposed scheme of feature extraction used the multi-level coefficients of decomposition parts of normalized iris image via 2D-CWT. The proposal is implemented using a dual-tree structure[69] and combined this technique with 2D Dual Tree Rotated Complex Wavelet Transform (RCWT). This method provides features in 12 directions against 3 and 6 directions in DWT and 2D-CWT respectively. Iris features are obtained by computing energies and standard deviation of detailed coefficients in 12 directions per stage, at 3 levels of decomposition.

A region-based feature extraction method based on 2D-Discrete Wavelet Transform was proposed by Tajbakhsh Misaghian et al.[70]. The normalized iris image is divided in to 32×32 pixel blocks with 50% overlap in both directions and then the 2D wavelet decomposition is performed one very block. Through an optimization process on the training set, six wavelet coefficients with the most discriminating power less affected by the degradation factors are selected.

Chen and Chu[71] used one dimensional circular ring to represent iris features. First, iris images are segmented and projected onto 1-D signals by the vertical projection. Then, the 1-D signal features are extracted by the 1-D wavelet transform.

In Harjoko Hartati et al.[72], they used one dimensional wavelet transformation. First, the iris area is converted into 1D form by dividing the iris area into 5×5 pixel blocks. Then, the mean intensity of each block is calculated in a left to right and top to bottom form. Each signal is transformed using 2^{nd} order Coiflet wavelet transformation with four decomposition levels. In each decomposition level, the wavelet transformation divides the signal into approximation signals and detail coefficients. In this method, the 4^{th} level approximation coefficients are used to represent the iris. To reduce the code size and the similarity measurement process, all coefficients are stored in integer form.

Pschernig[50] implemented two iris recognition algorithms, Zhu et al. algorithm[66] and Ma et al. algorithm[61], which used wavelets for feature extraction. In the new version of the algorithms, the wavelet parameters are used as a key when matching a new iris code, the correct key is needed for feature extraction in order to authenticate positively.

Nasare, Hase et al.[73] used complex wavelet and calculated different coefficient vectors. Complex wavelets transforms used complex valued filtering that decomposes the real/complex signals into real and

imaginary parts in transform domain. Particularity complex frequency B-spline wavelet is used for iris feature extraction. A complex frequency B-spline wavelet is defined by Eq.15 :

$$\Psi(x) = \sqrt{f_b}(\left(\sin c(\frac{f_b x}{m})\right)^m e^{2i\pi f_e x} . \tag{15}$$

Sachane and Jain[74] investigated the use of wavelet maxima components as a multi-resolution technique alternative for iris feature extraction. The proposed algorithm at each scale s decomposes the normalized iris image $I(x,y)$ into $I(x,y,s), W_v(x,y,s)$ and $W_h(x,y,s)$. At each scale $s(s = 0$ to $s = S-1)$, where S is the number of scales or decomposition image $I(x,y)$ is smoothed by a low-pass filter Eq.16 .

$$I(x,y,s+1) = I(x,y,s) * (H_s, H_s)) . \tag{16}$$

The horizontal and vertical details are obtained respectively by Eq.17 .

$$\begin{aligned} W_h(x,y,s) &= \frac{1}{\lambda_s} I(x,y,s) * (G_s, D) , \\ W_v(x,y,s) &= \frac{1}{\lambda_s} I(x,y,s) * (D, G_s) , \end{aligned} \tag{17}$$

where D is the Dirac filter whose impulse response is equal to 1 at 0 and 0 otherwise. The $A * (H,L)$ is the separable convolution of the rows and columns, respectively, of image A with the 1-D filters H and L.G_s and H_s are the discrete filters obtained by appending $2^s - 1$ zeros between consecutive coefficients of H and G. λ_s is the wavelet modulus maxima of a step edge do not have the same amplitude at all scales as they should in a continuous model. The constants λ_s compensate for this discrete effect.

Zero Crossings of the 1D Wavelet

The method developed by Boles and Boashash[75] represents features of the iris at different resolution levels based on the wavelet transform zero-crossing. The mother wavelet is defined as the second derivative of a smoothing function $\theta(x)$. The zero crossings of dyadic scales of these filters are then used to encode features. The wavelet transform of a signal $f(x)$ at scale s and position x is given by Eq.18 :

$$\begin{aligned} W_s f(x) &= f * \left(s^2 \frac{d^2 \theta(x)}{dx^2}\right)(x) \\ &= s^2 \frac{d^2}{dx^2}(f * \theta_s)(x) , \end{aligned} \tag{18}$$

where,

$$\theta_s = (1/s)\theta(x/s) , \tag{19}$$

$W_s f(x)$ is proportional to the second derivative of $f(x)$ smoothed by $\theta_s(x)$ and the zero crossings of the transform correspond to points of inflection in $f * \theta_s(x)$.

Martin-Roche, Sanchez-Avila et al.[76] and Sanchez-Avila and Sanchez-Reillo[77] presented an approach similar to that of Boles and Boashash. They encode the iris texture by considering a set of 1D signals from annular regions of the iris, taking a dyadic wavelet transform of each signal, and finding zero-crossings[16].

Hoyle, Feitosa et al.[78] presented an extension to Bole‘s method that it less sensitive to occlusion than its original formulation. The basic idea consists in restricting the computation of dissimilarity to the values

of the wavelet transforms not influenced by occlusion. Because the wavelet transform is a neighborhood operation, that is affected by the occlusion of a range extending beyond the pixels directly under occlusion. It includes the occluded pixels themselves and the pixels lying in a neighborhood of size w, where w is the width of the wavelet kernel. The wavelet used was taken from the Gaussian derivatives family, first derivative of the Gaussian probability density function.

Haar Wavelets Filter

Haar wavelet transform is the simplest wavelet used to extract features from the iris region. Haar wavelet function $\Psi(x)$ and its scaling function $\varphi(t)$ are defined as Eq.20 [79]:

$$\Psi(t) = \begin{cases} 1 & \text{si} \quad 0 \leq t < 1/2 \\ -1 & \text{si} \quad 1/2 \leq t < 1 \\ 0 & otherwise\ . \end{cases} \tag{20}$$

The Haar wavelets can capture sharp discontinuities in the spatial gray-level texture by repeated application of following low-pass (g) and high-pass (h) filters Eq.21 :

$$g = \frac{1}{\sqrt{2}}[1 \quad 1], h = \frac{1}{\sqrt{2}}[1 \quad -1]\ . \tag{21}$$

The above filters are separately applied to the rows and columns of the iris images resulting in four channel filter bank with channels low low (LL), low high (LH), high low (HL), and high high (HH) corresponding to filters $g^t * g, g^t * h, h^t * g$, and $h^t * h$ respectively. The recursive application of this decomposition is used to construct higher level decomposition[80].

Kwanyong, Shinyoung et al.[81] extracted features using the four-level Haar wavelet decomposition. The diagonal coefficients of the fourth level were employed to obtain 4×32 real values. In addition to these 128 values, the average of diagonal coefficients from the first, second and third level decomposition were also employed. Each of those 131 (3 + 128) values were quantized to binary values by simply converting the positive values to 1 and negative values to 0. Therefore, the feature vector for any iris constituted of only 131 bits[80].

In Daouk, El-Esber et al.[82], the enhanced images are decomposed into 5 levels by the Haar wavelets. Next the vertical, horizontal and diagonal coefficients of 4^{th} and 5^{th} level were employed. The coefficients of $1^{st}, 2^{nd}$, and 3^{rd} level were almost the same as those of the 4^{th} level and therefore the smallest of them (4^{th} level coefficients) were employed and the rest were ignored. The 5^{th} level decomposition offered the most discriminative information and therefore all the coefficients from this decomposition were employed. The phase encoding from the zero crossings of the coefficients formed the binary values of the feature vector. The size of this feature vector was 3 times the size of features of 4^{th} level (4×32) plus 3 times the features of 5^{th} level (2×16), therefore in total the size of feature vector was 480 bits[80].

In Tze Weng, Thien Lang et al.[83], they proposed an iris recognition system used a basic and fast Haar wavelet decomposition method. First the iris image contrast is enhanced using histogram to enable a better extraction of pattern by transforming the values in an intensity image. After histogram equalization, iris region is then decomposed using Haar decomposition up to four levels, only chosen to take the fourth level to reduce the code length (348 coefficients). These numbers are then converted to binary iris code converting positive coefficients to 1 and negative coefficients to 0.

In Panganiban, Linsangan et al.[84], the authors used wavelet transform to extract the discriminating information in an iris pattern. They experimented with two mother wavelets, Haar and Biorthogonal. The image was decomposed using the wavelets at N levels, where 4 is the maximum level. The wavelet transform breaks an image down into four sub-samples or images. The results consist of one image that

has been high-pass filtered in the horizontal and vertical directions, one that has been low-pass filtered in the vertical and high-pass filtered in the horizontal, and other that has been low-pass filtered in both directions. The experiment showed that Haar wavelet decomposed at Level 4 obtained the best results.

Birgale and Kokare[85] proposed the use of texture and color for iris recognition systems and reduced feature vector size of just 1×3. Pre-designed masks are used to filter out each eye image. Three levels wavelet decomposition is used for every filtered image to obtain texture content of an iris. They have used Haar wavelet coefficients giving comparatively good results. Histograms are used for color content extraction from an iris. Masks are used to avoid normalization step.

In Narote, Narote et al.[86], they used different mother wavelet: Haar, Daubechies, Coiflet, Symlet and Biorthogonal. They composed the normalized image using a fifth level decomposition. In order to create the feature vector they tried different combinations of HH level 5 (HH5), HL level 5 (HL5), and LH level 5 (LH5). The results obtained from different combinations are compared to find the best result. The binary feature vector is generated by quantizing the feature vector obtained by different combinations of HH5, HL5 and LH5. The binary feature vector is encoded by using two level quantization.

Kekre, Sudeepet al.[5] presented a novel Haarlet Pyramid based iris recognition using the image feature set extracted from Haar Wavelets at various levels of decomposition. The procedure of generating Haarlets is shown in Fig.6.

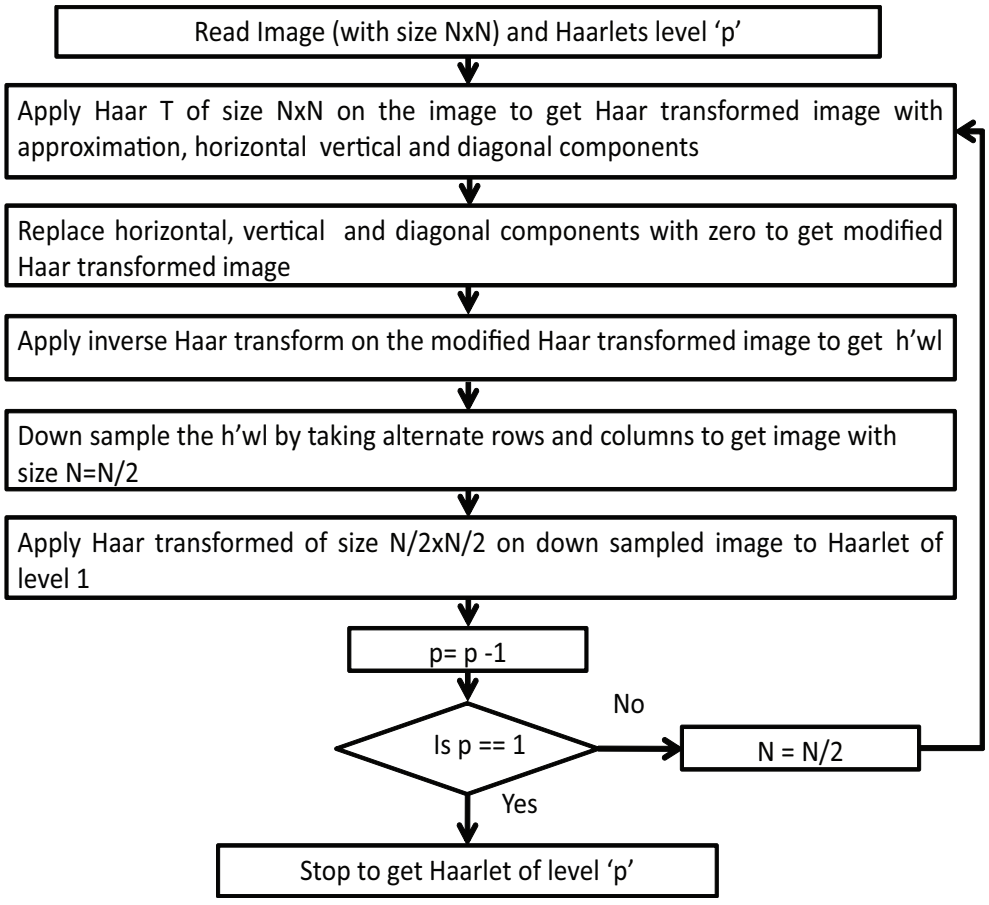

Fig. 6. Flowchart for generating Haarlets of level 'p' proposed by Kekre, Sudeepet al.[5].

Here the approximate components of Haarlet level-1, Haarlet level-2,....,Haarlet level-7 are obtained for every image in the database and Haar transforms of respective sizes are applied on them, the results are stored as feature vectors for respective image. At level-1 Haarlet the feature vector size is $N/2 \times N/2$. At level-2 Haarlet the feature vector size is $N/4 \times N/4$ and so on. Thus the feature vectors for up to level-7 Haarlets are extracted and the feature vector database is generated.

Wavelet Packets

Wavelet packets may be described by the collection of functions $\{W_j(x)|j \in Z^+\}$ obtained from Eq. 22:

$$\begin{aligned} 2^{\frac{p-1}{2}} W_{2n}(2^{p-1}x - \iota) &= \sum_m h_{m-2\iota} 2^{\frac{p}{2}} W_n(2^p x - m) \ , \\ 2^{\frac{p-1}{2}} W_{2n+1}(2^{p-1}x - \iota) &= \sum_m g_{m-2\iota} 2^{\frac{p}{2}} W_n(2^p x - m) \ , \end{aligned} \tag{22}$$

where p is a scale index, ι is a translation index, $W_0(x) = \phi(x), W_1(x) = \psi(x), \phi(x)$ is a scaling function and $\psi(x)$ is a basic wavelet. The discrete filters h_k and g_k are quadrature mirror filters[87].

Wavelet packet analysis is an extension of the DWT and it turns out that the DWT is only one of the much possible decomposition that could be performed on the signal[64]. The advantage of wavelet packet analysis is that it is possible to combine the different levels of decomposition in order to achieve the optimum time-frequency representation of the original[88].

Rydgren, Thomas et al.[89] used wavelet packet analysis to the features extraction part of an iris recognition system. An energy measure is used to identify the particular packet that carries discriminating information about the iris texture. They used 3-level wavelet packet decomposition that generates 64 output sub images, each representing a part of the frequency plane.

In Gan and Liang[90] the authors, firstly divided iris image into several windows, and Wavelet Packets Decomposition (WPD) is done to them. Daubechies-4 wavelet decomposition is adopted, and each window of iris image is divided into 3 levels. In order to maintain effective information, get rid of the redundancy and diminish the effect of noise, LL3 , HL3 , LH3 , HL2 and HL1-LL altogether 5 subband images are held as the feature extraction objects. Secondly, the farther feature extraction and compression are applied to these sub-band images by way of Singular Value Decomposition (SVD), and iris recognition features are obtained. Finally, Weighted Euclidean Distance (WED) classifier is used in recognition.

In the work of Lokhande and Bapat[91] wavelet packet decomposition is applied to iris images using Daubechies-2 wavelet packets filters with energy. They integrate the energy values of each subband of the wavelet packet decomposed iris image.

Lokhande and Vishram[92] used wavelet packet decomposition of 50 $\times$ 250 size. The normalization of iris images is carried out up to level 3 using Haar wavelet. This generates 64 packet subimages each of size 7$\times$32. Then, an energy (E) see Eq.23, based criterion describes information related properties for accurate representation of texture information in packet sub-images and computed as below:

$$E = \sum_x \sum_y |f(x,y)|^2 \ . \tag{23}$$

Others Wavelets Transform

Lifting wavelet transform is a technique used to construct DWT using lifting steps. In this process, the signal is split into odd and even samples. In the predict step, odd samples are predicted from the even samples. In the update step, even samples are updated from the input even samples and updated odd

samples[79]. Patil and Patilkulkarani[93] used Lifting wavelet Transform to extracts the important features from the iris image. They followed three steps to decompose signal, that is, Split, Predict and Update:

1. Split: In this step, the original signal $s[n]$ is split into two subsets which do not overlap with each other: $se[n]$ (even sequence) and $so[n]$ (odd sequence), that is:

$$\begin{aligned} s_e[n] &= s[2n] \ , \\ s_o[n] &= s[2n+1] \ . \end{aligned} \tag{24}$$

2. Predict: If the original signal is locally coherent, the subsets $se[n]$ and $so[n]$ are also coherent, so one subset can be predicted by another. Commonly we use even sequence to predict odd sequence:

$$d[n] = s_o[n] - P(se)[n] \ , \tag{25}$$

   where P is the predict operator and reflects the degree of correlation of data. $P(se)[n]$ implies that the value of $d[n]$ can be predicted by the value of $se[n]$.
3. Update: $c[n]$ is the approach signal which has been decomposed. One of the important features is that its average value should be equal to the average value of original signal $s[n]$. So we can use detail subset $d[n]$ to update the signal $se[n]$, expressed by $c[n]$:

$$c[n] = se[n] + U(d)[n] \ . \tag{26}$$

Rampally[79] also used the same tecnique explain above to construct DWT. In this process, the signal is split into odd and even samples. In the predict step, odd samples are predicted from the even samples. In the update step, even samples are updated from the input even samples and updated odd samples. In this method the iris template has been divided into 20×20 blocks and Lifting Wavelet transform is applied to each block. Each block is divided into 4 sub bands denoted by LL, LH, HL, and HH.

Zhonghua and Bibo[94] used one dimension Morlet wavelet transform row by row to the iris image in the effective iris area, gets a series of wavelet transform real coefficients of different scales and gets the distribution figure of these coefficients of different scales.

Khalighi, Tirdad et al[95] proposed new scale, shift and rotation invariant feature extraction method for iris recognition in non-subsampled contourlet transform domain (NSCT). In contourlet transform, the Laplacian Pyramid (LP) is first used to capture point discontinuities, and then followed by a Directional Filter Bank (DFB) to link point discontinuities into linear structures. The overall result is an image expansion using basic elements like contour segments, and thus called contourlet transform, which is implemented by a Pyramidal Directional Filter Bank. The LP decomposition at each level generates a down sampled low pass version of the original image, and the difference between the original image and the prediction results in a bandpass image. Due to down-sampling an dup-sampling presented in both LP and DFB, contourlet transform is not shift-invariant. The NSCT is built upon non-subsampled pyramids and non-subsampled directional filter bank (NSDFB); thus, it is a fully shift-invariant, multi-scale, and multi-direction image decomposition that has a fast implementation.

2.5. Discrete Cosine Transform

The Discrete Cosine Transform (DCT) is a real valued transform, which calculates a truncated Chebyshev[6] series possessing well-known mini max properties and can be implemented using the Discrete Fourier

[6] Chebyshev Interpolation: An Interactive Tour in http://www.maa.org/publications/periodicals/loci/joma/chebyshev-interpolation-an-interactive-tour

Transform (DFT). There are several variants, but the one most commonly used operates on a real sequence *xn* of length N to produce coefficients C_k, as follows Eq.28 [96]:

$$C_k = \frac{2}{N} w(k) \sum_{n=0}^{N-1} x_n \cos(\frac{2n+1}{2N}\pi k), 0 \leq k \leq N-1 \ , \tag{27}$$

and

$$x_n = \sum_{k=0}^{N-1} w(k) C_k \cos(\frac{2n+1}{2N}\pi k), 0 \leq k \leq N-1 \ , \tag{28}$$

where

$$w(k) = \begin{cases} \sqrt{2} \text{ si } k = 0 \\ \\ 1 \text{ si } x < 1 \leq k \leq N-1 \ . \end{cases}$$

Alim and Sharkas[97] try four different methods: a Gabor phase coefficients, an histogram of phase coefficients, a four- and six-level decomposition of the Daubechies wavelet and a discrete cosine transform (DCT). The output of each feature extraction method is then used to train a neural network. The best performance, at 96% recognition, was found with the DCT and a neural network with 50 input neurons and 10 hidden neurons[16].

In Monro, Rakshit et al.[98] they started from a general paradigm where feature vectors will be derived from the zero crossings of the differences between 1D DCT coefficients calculated in rectangular image patches. Averaging across the width of these patches with appropriate windowing helps to smooth the data and mitigate the effects of noise and other image artifacts. It then enables us to use a 1D DCT to code each patch along its length, giving low-computational cost. The selection of the values for the various parameters was done by extensive experimentation over the CASIA and Bath databases to obtain the best predicted Equal Error Rate (EER). The two data sets were used in their entirety to optimize the parameters of the method.

Dhavale[99] proposed a new iris feature extraction technique based on the statistical properties of DCT domain. The main steps of this proposal are:

1. DWT is applied on the previous segmented and normalized iris region to get approximation and detail coefficients. Haar wavelet is used as the mother wavelet. The 2D DWT leads to a decomposition of approximation coefficients at level j in four components: the approximation at level $j+1$, and the details in three orientations (horizontal, vertical, and diagonal).
2. Both subbands are first segmented into non-overlapping 8x8 non-overlapping blocks. Apply DCT to each of the 8×8 block of both subbands. The energy-compaction characteristics of DCT in both subbands are used further to capture iris texture variations.
3. Calculate the energy of each 8×8 DCT block for both the subbands as Eq.29:

$$\begin{aligned} HE_k &= \frac{1}{N_k} \sum_{i=1}^{N_k-1} \|DH_k\|^2 \\ VE_k &= \frac{1}{N_k} \sum_{i=1}^{N_k-1} \|DV_k\|^2 \ , \end{aligned} \tag{29}$$

where, HE_k is energy of k_{th} DCT block of Horizontal detail wavlet subband, VE_k is energy of k_{th} DCT block of Vertical detail wavlet subband and $N_k = 64$ is total number of DCT coefficients in each block vector.

4. Form binary image template using both subband energy vectors representing iris texture variations using the following criteria. For a k_{th} block, if HE_k is greater than VE_k then set all pixels of corresponding 8×8 block of binary template as 255 i.e. all white pixels. Else set all pixels of corresponding 8×8 block binary template as 0 i.e. all black pixels.
5. Form final binary bit stream/unique code B corresponding to above binary iris image template.
6. Further to increase the security of the system, the above binary bit stream B is first encrypted using the user key.

In Mehrotra, Srinivas et al.[100] the features are extracted from the preprocessed image using multi-resolution DCT. The input iris strip is divided into non-overlapping 8×8 pixel blocks which are transformed to generate DCT coefficients. Each block of the computed DCT coefficients has to be reordered to form subbands like 3 level wavelet decomposition. The block of size 8×8 is reordered to transform coefficients into multi-resolution form. After reordering all the DCT blocks, the coefficients from each block belonging to a particular subband are grouped together. Energy of each subbandis obtained by summing up the square of coefficients. The reason behind using block based DCT approach is that it extracts local texture details of an image. It has been observed that multi-resolution decomposition provides useful discrimination between texture

2.6. Combined Method

2.6.1. Log Gabor-Wavelet

Masek[48] convolved the normalized iris pattern with 1D Log-Gabor wavelets. The 2D normalized pattern is broken up into a number of 1D signals, and then these 1D signals are convolved with 1D Gabor wavelets. The rows of the 2D normalized pattern are taken as the 1D signal; each row corresponds to a circular ring on the iris region. The angular direction is taken rather than the radial one, which corresponds to columns of the normalized pattern, since maximum independence occurs in the angular direction.

Popescu-Bodorin and Balas[101] designed a faster and simpler variant of the encoder designed originally by Masek. Their version is a single-scale one dimensional Log-Gabor filter. Each line of the unwrapped normalized iris segment situated in the angular direction is convolved with 1-D Log-Gabor Wavelet Eq. 30:

$$G(f) = exp[-\frac{0{,}5\log^2(\frac{f}{f_0})}{log^2(\frac{\sigma}{f_0})}] \,, \tag{30}$$

where f_0 and σ represent the center frequency and the bandwidth of the filter. Prior to the Log-Gabor filter they don't make any enhancement of the iris texture.

Patil, Kolhe et al. [12] constructed filters in the frequency domain using a polar co-ordinate system. On the linear frequency scale, log-Gabor has a transfer function of the form Eq.31:

$$g(f) = e^{\frac{-(\log(\frac{f}{f_0}))^2}{2(log(\frac{\sigma}{f_0}))^2}} \,, \tag{31}$$

where f_0 is the centre frequency of filter and σ is the bandwidth of filter.

If $I(x,y)$ denoted the image and W_n^e and W_n^0 denote the even symmetric (cosine) and odd-symmetric (sine) wavelets at a scale *n*, we can think of the responses of each quadrature pair of filters as forming a response vector Eq. 34,

$$[en(x,y), on(x,y)] = [I(x,y) * W_n^e, I(x,y) * W_n^0] \,. \tag{32}$$

The amplitude of the transform at a given wavelet scale is given by

$$An(x,y) = \sqrt{en(x,y)^2 + on(x,y)^2} \ , \tag{33}$$

and the phase is given by

$$\phi n = \alpha \tan 2(en(x,y), on(x,y)) \ , \tag{34}$$

where $An(x,y)$ is the amplitude and ϕn is the phase of the angle. During the phase extraction, the iris image is divided into m by n blocks. Consequently, information in each block is encoded into 2-bit codes. Thus the phase information in each block is described by 2-bit codes and totally $2 \times m \times n$ bits to describe the whole iris.

Anand, Tiwari et al. [102] proposed the use of log polar form of 1D Gabor wavelet for iris texture template. Like Gabor wavelets, log polar Gabor filters are based on polar coordinates but unlike the frequency dependence on a linear graduation, the dependency is realized by a logarithmic frequency scale.

Peng-Fei De-Sheng et al. [103] described a system that encode both global and local texture information using a log-Gabor wavelet filter. The global features are intended to be invariant to iris rotation and small errors in localization. The local features are essentially the normal iris code[16].

2.6.2. 2D Gabor-Wavelet

It is possible to represent images on a sparse self-similar family of primitives with advantageous reductions in complexity by eliminating degrees of freedom in the family of 2-D Gabor elementary functions, so that they all are dilations, rotations, and translations of each other, with the spectral parameters of the set distributed in a 2-D log-polar lattice. This set of elementary functions can form a complete self-similar wavelet expansion basis[104].

If take $\Psi(x,y)$ to be a chosen generic 2-D Gabor Wavelet, then can generate from this number, a complete self-similar family of 2-D wavelet through the function Eq. 35:

$$\Psi_{mpq\theta}(x,y) = 2^{-2m}\Psi(x',y') \ , \tag{35}$$

where the substituted variable (x',y') incorporate dilations of the wavelet in size by $2^{(-m)}$, translations in position (p,q), and rotations through angle θ Eq.36:

$$\begin{aligned} x' &= 2^{-m}[x\cos(\theta) + y\sin(\theta)] - p \ , \\ y' &= 2^{-m}[y\cos(\theta) - x\sin(\theta)] - q \ . \end{aligned} \tag{36}$$

Daugman exploited this self-similarity properties of 2D Gabor filters in analyzing textures across multiple scales to construct identification codes[6]. The paired real and imaginary parts of 2D Gabor wavelets can be used to construct a phase demodulation code (IrisCode), see Fig. 7. The angle of each phasor is quantized to one of the four quadrants when a given area of the iris is projected onto complex-valued 2D Gabor wavelets Eq.37. This process is repeated all across the iris with many wavelet sizes, frequencies, and orientations to extract 2048 bits[105].

$$h_{\{Re,Im\}} = sng_{\{Re,Im\}} \int_{\rho}\int_{\phi} I(\rho,\phi) e^{-iw(\theta_0-\phi)} e^{-(r_0-\rho)^2/\alpha^2} e^{-(\theta_0-\phi)^2/\beta^2} \rho d\rho d\phi \ . \tag{37}$$

Nabti and Bouridane[7] combined multi-resolution iris feature extraction scheme by analyzing the iris, using first wavelet maxima components and then applying a special Gabor filter bank to extract all dominant features. Their method includes the following steps:

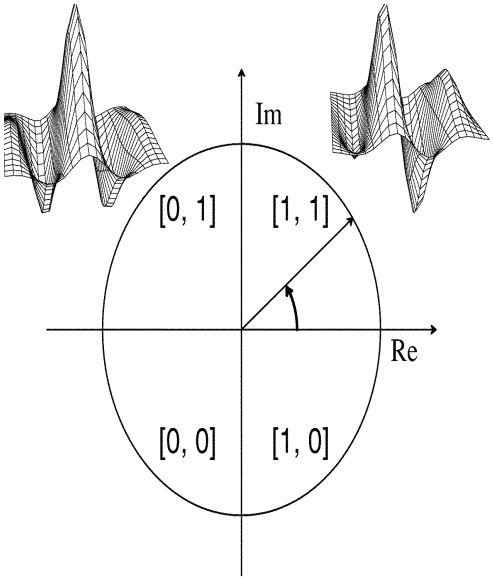

Fig. 7. Phase demodulation code proposed by Daugman[6].

1. Compute wavelet maxima components in horizontal and vertical directions using five scales.
2. For each component, special Gabor filter bank is applied with 4 scales and 6 orientations to obtain $((4\times 6)\times 5)\times 2 = 120\times 2 = 240$ filtered image.
3. The feature vector is presented by using two different techniques, the first is a statistical measure (mean and variance) and the second technique is moment invariants Fig. 8.

In the proposal of Salih and Dhandapani[106] the normalized iris image is divided into multiple regions. Each local region is transformed in to a complex number with 2-D Gabor filters.

The authors Gulmire and Ganorkar[107] firstly construct two-dimensional Gabor filter, and take it to filter these images. After get phase information, they code it into 2048 bits, i. e. 256 bytes. In image processing, a Gabor filter, named after Dennis Gabor Eq.38, is a linear filter used for edge.

$$G\imath p_{r_o\theta_o} = exp^{(-2\pi^2\sigma^2(\imath n\frac{r-r_0}{f})^2\tau^2)/(2\ln(f_0\sin(\theta-\theta_2))^2)}\,, \tag{38}$$

where (r,θ) are the polar co-ordinates, r_0 and θ_0 are the initial values, f is the center frequency of the filter and f_0 is the parameter which controls the bandwidth of the filter, σ and τ are defined as follows Eq. 39:

$$\begin{aligned}\sigma &= \frac{1}{\pi\ln(r_0)\sin(\pi/\theta_0))}\sqrt{\frac{\ln 2}{2}}\,,\\ \tau &= \frac{2\ln(r_0)\sin(\pi/\theta_0)}{\ln 2}\sqrt{\frac{\ln 2}{2}}\,.\end{aligned} \tag{39}$$

In Belcher and Du[108] and Du, Belcher et al. [109]; the Gabor wavelet is incorporated with scale-invariant feature transformation (SIFT) for feature extraction to better extract the iris features. Their method includes the following steps:

1. Feature Subregion Maps: They divided the iris area into a fixed number of subregions, and ensure each region has at most one feature point. In this way, for each feature point, they know its subregion and

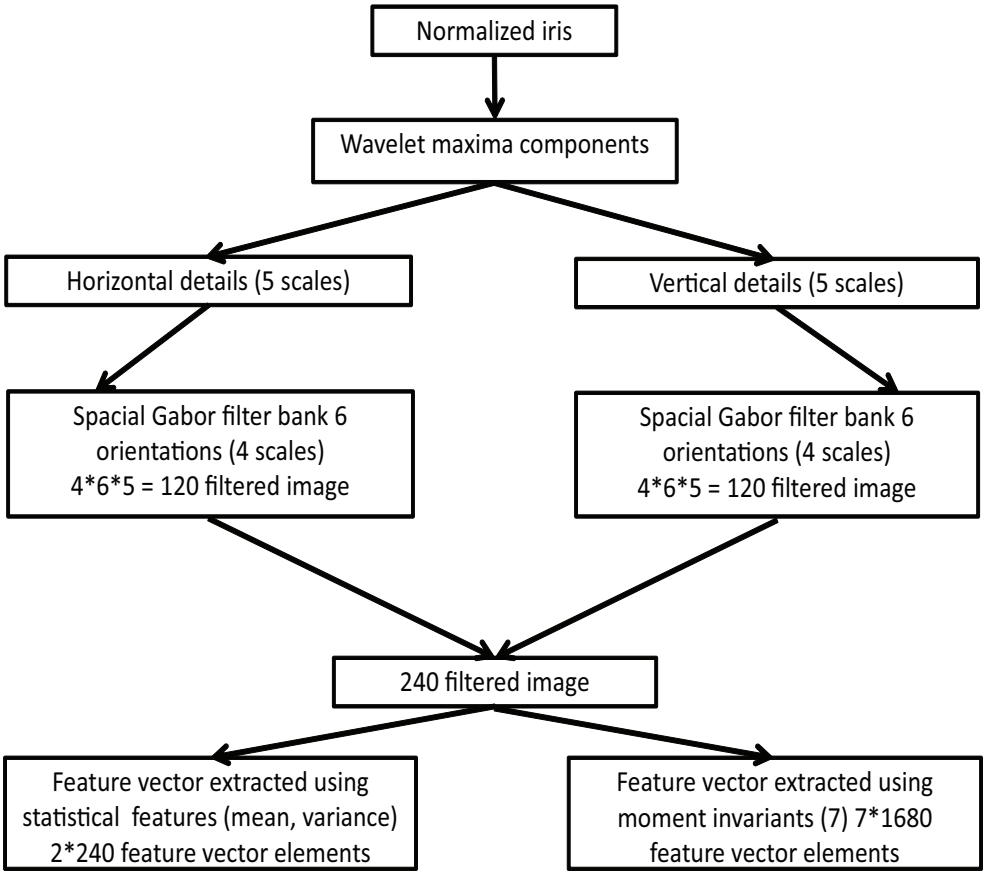

Fig. 8. Combined multiscale feature extraction technique diagram proposed by Nabti and Bouridane.[7].

the correlation of the subregion to other subregions. Therefore, we have the global information of the feature points for matching.

2. Feature Point Selection: They used the SIFT and Difference of Gaussian (DoG) approach to find potential feature points[110].
3. Feature Description: For each feature point, a feature description of length 64 is created based on the normalized and Gaussian weighted position of each point within a normalized window around a feature point (4 x-bins and 4 y-bins) and the magnitude and phase response (4 phase orientation bins).
4. Region-Based Matching: To match two iris images, the set of two 10 by 72 feature point maps are compared and the Euclidean distance is found between each feature point descriptor.

Park and Park[111] used their pervious work Jeong, Park et al. [60] for local and global iris texture extraction and the Hamming Distance calculated by Gabor filters, fused by the SVM. Shin, Nam et al. [112] applied this Filter to gray, red, and green channels to afford three separate iris codes. This work obtained four placed in NICE. II iris biometrics competition.

2.6.3. Combination of Ordinal Features

Tan, Zhang et al.[8] proposed an integrated scheme to match visible light iris images in uncontrolled situations. As shown in Fig. 9. , it consists of image preprocessing, feature extraction, matching, and multi modal fusion. First, the original input data are preprocessed to obtain the normalized iris data and eye

data. Secondly, ordinal measures and color histogram are computed to characterize iris data, and texton representation and semantic label are used as eye patterns. Thirdly, four matching scores are obtained by different matching algorithms, namely SOBoost learning for ordinal measures, diffusion distance for color histogram, chi-square X^2 distance for texton representation, and exclusive OR operator (XOR) for semantic label. Finally, a robust score level fusion strategy is applied to generate the final dissimilarity score. This work takes first place in NICE. II iris biometrics competition.

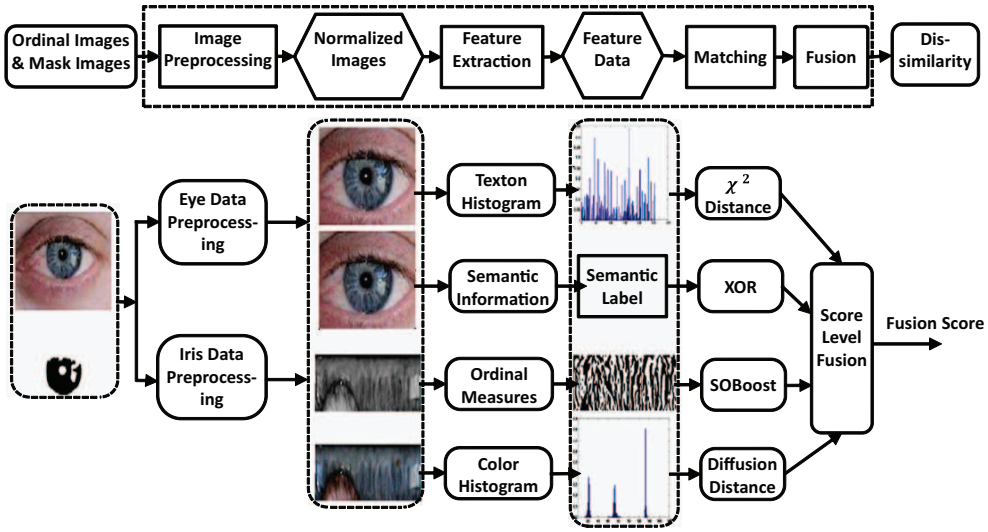

Fig. 9. Flowchart of the proposed method Tan, Zhang et al.[8].

Zhang, M., Z. Sun, et al.[113] proposed a novel deformed iris image matching method using bandpass geometric information and lowpass Ordinal features to address deformed iris image matching problem. The main steps of this proposal are:

- Firstly, normalized iris image are decomposed into lowpass and bandpass sub-bands by nonsubsampled contourlet transform[114] (first level stands for the lowpass subband and the other ones represent bandpass in 8 orientations).
- Secondly, bandpass subbands are taken to construct maxima images [$M(i,j) = max(D_n(i,j))$ where D_n is the difference between two subbands in each direction, M is maxima image and (i,j) is the pixel coordinate] and extract key points [using Speed Up Robust Features,(SURF)] in order to align deformed iris image.
- Thirdly, the location of key point are utilized for aligned ordinal feature extraction in lowpass subbands.
- Finally these two sets of features in different subbands are fused.

The experimental result get better performance compare to gabor wavelet and ordinal features.

Li, X., L. Wang, et al.[115] proposed a method to off-angle iris recognition. The basic idea of they approach is to classify off-angle iris images into multiple categories according to the orientation of eye gaze (i.e., frontal, right, left, up and down) and then learn category-specific ordinal features to match distorted iris texture patterns. They adopt the Wang, Sun et al. [45] method's to choose features for different off-angle categories. The experimental result improve recognition performance even using simple ordinal features.

2.6.4. Other Proposed Methods

Balas, Motoc et al.[9] combined Haar-Hilbert with Log-Gabor filter as illustrated in Fig. 10.

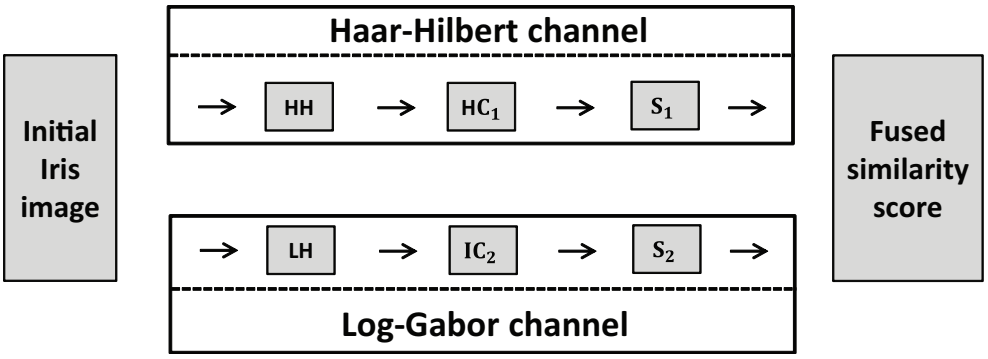

Fig. 10. Iris recognition based on classifier fusion and single eye enrollment scenario proposed by Balas, Motoc et al.[9].

Iris image *I* is acquired for the current candidate *C* and two candidate iris codes *IC*1 and *IC*2 are generated from the image *I* using the Haar-Hilbert and Log-Gabor encoders. Then the candidate iris codes *IC*1 and *IC*2 are matched against two binary templates stored under a certain claimed identity *E* using the Hamming distance and two similarity scores *S*1 and *S*2 are computed as the results of these comparisons.

Santos and Hoyle[10] proposed a novel fusion of different iris recognition approaches as schematized in Fig. 11. The method was tested at the NICE. II and performance was corroborated by the obtained third-place. They used 1-D wavelet zero-crossing, 2-D dyadic wavelet zero-crossing representation and comparison maps (is own extension Santos and Proenca[116] to the widely known Daugman method) to represent the feature iris code. The SIFT an LBP is used to represent features of the ocular region.

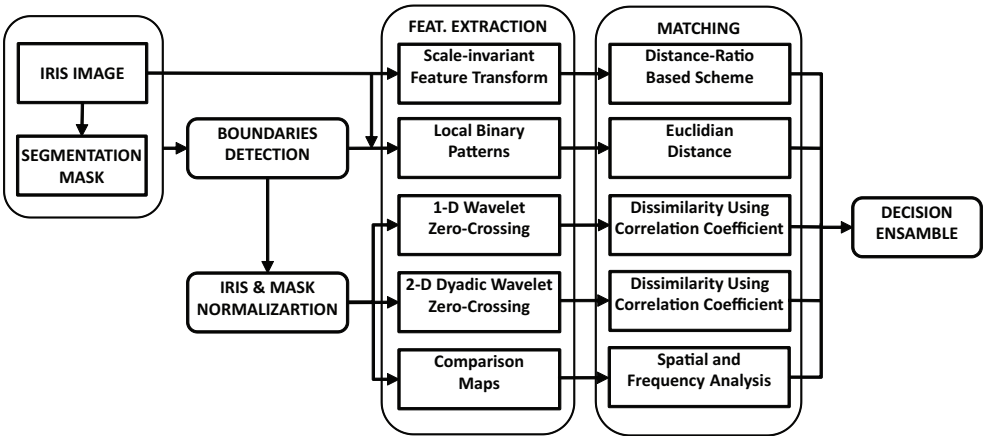

Fig. 11. Methodology proposed by Santos and Hoyle[10].

Gawande, Zaveri et al. [117] combined zero-crossing 1D wavelet (Bole's algorithm[118]), Euler No. and Genetic Algorithm (GA) based for feature extraction. The Euler No. extracted local topological features. For a binary image, the Euler No. is defined as the difference between the No. of connected components and the No. of holes. They represented each pixel of unwrapped iris as an 8-bit binary vector. GA selected the prominent features based on the outcomes of the four features selection algorithms, namely the Entropy based approach, k-NN based method, T-statistics and the SVM-REF approach. They used a hybrid approach to obtain the most selection algorithm subset from the different feature selection algo-

rithms. The output from these three algorithms is normalized and their score are fused to decide whether the user is genuine or imposter.

Feddaoui, Mahersia et al. [119] and Feddaoui, Mahersia et al. [120] proposed a novel method to extract iris features combining Gabor filters and uniform local binary patterns (ULBP) operators. The proposed process can be summarized as follows:

1. Represent global spatial texture information by application of a set of Gabor filters on iris image.
2. Compute ULBP operators in each filtered image to encode local variation crossing different Gabor coefficients around a defined radius.
3. Extract the global and local signatures, first, by dividing each obtained imageinto no overlapping blocks having a given size, then computing statistical featureswithin each block to form a vector.
4. Form iris template by encoding local relationship between measures of vector.

In works Kumar, Raja et al.[11] ; Kumar, Raja et al. [121], DWT and PCA are applied on iris template to derive iris features, and different classifiers are used for matching. See the pseudo-code below:

- Input: Eye image.
- Output: Recognition of a person.
- Step 1: Read the eye image.
- Step 2: Iris template creation.
- Step 3: Histogram equalization on the iris template.
- Step 4: The coiflet wavelet is applied and the approximation band is considered.
- Step 5: PCA is applied on approximation band to form feature vector.
- Step 7: Form the signature of each image.
- Step 8: Perform steps 1 to 7 for test image.
- Step 9: Match/Non match decision is obtained using multiclassifiers.

The PCA, known as Eigen XY analysis is applied on the approximation band of DWT to reduce the dimensionality of the image data. This technique extracts the main variations in the feature vector and allows an accurate reconstruction of the data to be produced from the extracted feature values and reduces the amount of needed computation. PCA identifies the strength of variations along different directions in the image data which involves computation of Eigen vectors and corresponding Eigen values. The Eigen vectors with largest associated Eigen values are the principal components and correspond to maximum variation in the data set, see Fig. 12.

3. Discussion

In this section some experimental results and conclusions about the analyzed topics are discussed.

In general it can be said that statistical methods are not much used for feature extraction in biometric iris recognition, but the few methods found showed good results.

The LBP are robust to rotation[25], can be used in combination with other local feature detectors[26] and achieve good results. Another known property is its low computational cost. This method presents problems when working with eye images captured at different scales.

The ICA algorithms are very effective when using very good quality iris images with a small size. In general, the results obtained by Bouraoui, Chitroub[31], allow us to concluded that ICA could perform well for such application. But the ICA algorithms are sensitive to illumination and noise degradations caused by the eyelids and eyelashes.

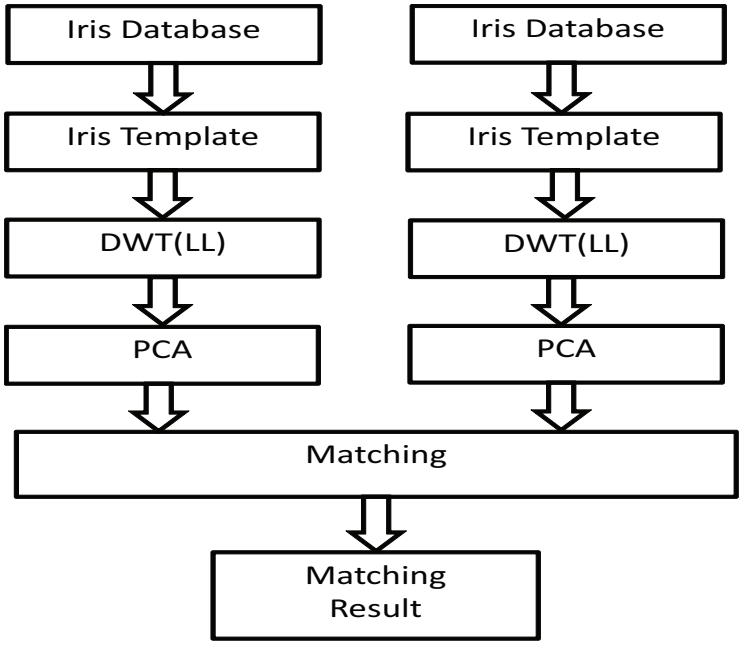

Fig. 12. Iris recognition flow diagram proposed by Kumar, Raja et al.[11].

The weighted co-occurrence phase histogram[27] is very distinctive and insensitive to illumination changes and noise. Besides, the proposed methods, give some robustness to alignment problems.

The methods proposed by Rathgeb and Uhl[33] is very simple, easy to implement and low computational cost. They experiments achieved good results.

Marsico, Nappi et al.[26] used two advantage (noise reduction and better blob setting off) of Laplacian of Gaussian filters an created BLOB. They combined BLOB whit LBP and archived good result NICE.II iris biometrics competition.

This study found several papers that extract color information using different strategies [52],[85],[3] and [112]. With the analysis carried out can conclude that: 1) the color information is not exploited to the fullest 2) color features are robust to the captured off-angle iris images, rotation and scaling problem [122] and 3) the use of various color spaces provide best results[123],[3].

The Daugman's method demonstrated the highest accuracy by using 2D Gabor wavelets. To achieve high accuracy, the size of each local region must be small enough, which result sin a high dimensionality of the feature vector (2048 components). His method captures much more information in much smaller local regions[7]. Besides, the Iriscode, has drawn considerable attention in the last years because of its commercial success, and outstanding performance in terms of speed and accuracy. Many coding methods that are very similar to the Iriscode have been proposed. A common approach is to substitute other linear transforms or filters for the Gabor filters in the Iriscode[124].

The 2D Gabor filter can be used in the patches of iris images[53] and extract local features, and then can be implement some classifier to select the best feature. 2D log-Gabor filter can be efficient in capturing global characteristics, resulting in a system with low false acceptance rates[59].

Patil, Kolhe et al.[12] compared feature extraction algorithm based on PCA, Log-Gabor wavelet and Gabor Wavelet, see Table 1. The results clearly demonstrate the effectiveness of the Daugman's method. With strict image quality control, Gabor filter based method is slightly better than the Log-Gabor wavelet

and PCA based methods. The authors also argue that the methods based on Log-Gabor wavelet can be tolerant to illumination variations.

Tabla 1. Experimental results proposed by Patil, Kolhe et al.[12].

Method	Feature Vector Length (Bits)	Classifier	Recognition Rate
Gabor Wavelet	2048	Recognition Rate	99%
Log Gabor Wavelet	1024	Recognition Rate	92.4%
PCA	1100	Euclidean Distance	90.2%

Bole's algorithm[118], zero-crossings, is invariant to translation, rotation, scale and illumination and can handle the noisy conditions as well. Martin-Roche, Sanchez-Avila et al. [76] and Sanchez-Avila and Sanchez-Reillo[77] demotrated, in their experiment, that the zero-crossings approach achieves even slightly higher performance over Daugman-like approach, using Gabor filtering. They also reported that the zero-crossings based approaches are faster than the Daugman-like approach.

Kwanyong, Shinyoung et al. [81] showed that Haar wavelet provides slightly better Recognition rate when compared with Gabor wavelet.

Rydgren, Thomas et al. [89] exposed that the wavelet packet approach can be a good alternative to the standard wavelet transform since it offers a more detailed division of the frequency plane. Lokhande and Vishram[92] used this method to show that wavelet packet is more suitable for the application within non cooperative images.

Vatsa, Singh et al. [125] implemented and compared four algorithms Daugman's method[126]; Ma's algorithm which uses circular symmetry filters to capture local texture information and create a feature vector[62]; Sanchez-Avila's algorithm[76] based on zero-crossings; and Tisse's algorithm[127] which uses emergent frequency and instantaneous phase. A comparison of the four algorithms, using the CASIA 1 database, showed that Daugman's algorithm performed the best with 99. 90% accuracy, then Ma's algorithm with 98. 00%, Avila's with 97. 89%, and Tisse's algorithm with 89. 37%[16].

Thornton, Savvides et al. [128] compared seven different filter types. They considered the Haar-wavelet, Daubechies wavelet of order three, Coiflet wavelet of order one, Symlet wavelet of order two, Biorthogonal wavelet, of order two and two, circular symmetric filters, and Gabor wavelets. They applied a single bandpass filter of each type and determined that the Gabor wavelet gave the best equal error rate. They then tuned the parameters of the Gabor filter to optimize performance. They concluded that Gabor wavelets are the most discriminative bandpass filters for iris patterns among the considered candidates, they noted that the performance of Gabor wavelet seems to be highly dependent upon the parameters that determine its specific form[16].

Sheela and Vijaya[129] showed that wavelet transformation is applied for the non-core components. The non-core components are the regions which show variations in the texture and intensity values. They implements different type of mother wavelets, Haar, db4, symlets, coiflets and biorthogonal. The results obtained using db4 are promising for recognition.

Kumar and Passi[80] investigated the comparative performance from four different approaches for the iris identification: DCT, FFT, Haar wavelet and Log-Gabor filter. Their experimental results suggest that the performance from the Log-Gabor filter is the best, which is followed in order by the Haar wavelet, DCT and FFT. Moreover, they also investigated the possible improvement of the performance using score-level combination. The experimental results suggest that the combination of Log-Gabor and Haar wavelet matching scores using weighted sum rule is the most promising. The Haar wavelet based approach is also the most attractive as it requires minimum computational time and can be easily implemented in fixed point environment.

The OMs for iris recognition proposed by Sun and Tan[40] showed excellent results compared to state of the art algorithms. Since Dr. Daugman's pioneer work, iris recognition accuracy has never been substantially improved because existing iris recognition methods are almost all limited to local image filtering, the OMs based on nonlocal differential filters break this limitation and illustrate the promising direction to improve iris recognition performance. Due to the easy implementation of OMs, fast algorithms of iris recognition can be developed for embedded systems such as mobile phones, PDAs, and digital cameras.

The investigations of iris feature extraction have considered a wide variety of filters to analyze the texture of the iris including 2D Gabor-wavelet, log-Gabor, Laplacian-of-Gaussian, DCT, etc. In accordance with Bowyer[16] can say that, there is not consensus on which types of filters give the best performance. Besides even though a number of papers make experimental comparisons, very little effort is made to test the observed difference in performance for statistical significance.

Table 2. originally proposed by[16] summarizes some of the conclusions reached in different studies, the table have been update with the main methods until 2013.

Tabla 2. Results of selected filter comparisons.

First author, year	**Operation found toper form the best**	**Compared to**
Alim[97], 2003	Discrete cosine transform	32 Gabor phase coefficients or Daubechies.
Du[130], 2006	2D log-Gabor	1D log-Gabor.
Krichen[131], 2004	Wavelet packets	Gabor wavelets.
Liu[132], 2006	Haar, Biorthogonal-1.1	Daubechies, Rbio3.1.
Rydgren[89], 2004	Gabor wavelets	Wavelet packets, Haar wavelets, Daubechies, Biorthogonal and others.
Sun[41], 2004	Robust direction estimation	Gabor filter, quadratic spline wavelet and discrete Haar wavelet.
Thornton[133], 2005	Correlation filters	1D log-Gabor and 2D Gabor.
Thornton[128], 2007	Gabor wavelets	Haar, Daubechies, Coiflet, Symlet, Biorthogonal, Circular Symmetric.
Peng[56], 2006	Modified log-Gabor	Complex Gabor filters used by Daugman.
Sun[40],2009	Ordinal Measures	Complex Gabor filters used by Daugman,1-D wavelet transform.
Lu[38],2008	Laplacian of Gaussian	Complex Gabor filters used by Daugman,Gabor filter.
Hoyle[78], 2009	Zero Crossings of the 1 D Wavelet	Wildes's methods, 1-D wavelet transform, 1D DCT and others.
Bastos[59], 2010	2D log-Gabor	Maseks methods, 1D log-Gabor
Rashad[1], 2011	LBP and combined LVQ	Wildes's method, Masek's method, Daugman's method, LBP + Histogram + LVQ, LBP + Histogram + combined LVQ classifier n = 3.
Panganiban[84], 2011	Haar and Biorthogonal Wavelet	Haar and Biorthogonal Wavelet at different level of decomposition.
Bouraoui[31], 2012	Independent Component Analysis	Ma's methods[61][67], JADE, Fast-ICA, Newton-ICA.
Lokhande[92],2013	wavelet packet (level 3 using Haar wavelet)	Daugman's method, Boles's method[75].

One important current research emphasis is the acquisition of images under less constrained conditions. There are various factors into the concept of less controlled circumstances, such as light reflection,

illumination change, eyelashes, eyelids,ect. The second phase of the NICE competition 2010 evaluated the performance of algorithms for feature extraction and matching in this environment. The Table 3. summarized the eight, best-ranked algorithms.

Tabla 3. Eight best-ranked algorithms in NiceII competition.

No.	Method	Author	Feature extraction technique	Description
1	Integrated Scheme	Tan, Zhang et al. 2012	Ordinal measures and color histogram for Iris texture. Texton representation and semantic label eye patterns.	Ordinal measures and color histogram are computed to characterize iris data, and texton representation and semantic label are used as eye patterns. Four matching scores are obtained by different matching algorithms. Robust score level fusion strategy is applied to generate the final dissimilarity score.
2	Adaboost-2D Gabor	Wang, Zhang et al. 2012	2D Gabor.	Constructed feature set based on 2D-Gabor for whole iris and patches. Adaboost learning is used for accurately and inaccurately segmented irises separately.
3	Fusion Approach	Santos and Hoyl. 2012	1D wavelet and 2D wavelet zero-crossing for Iris texture. LBP and SIFT point for ocular region.	Both 1D wavelet and 2D wavelet zero-crossing maps are used as representations of Iris texture. Used the iris code resulting from 2D Gabor filters, but viewed as a binary ”map” of the image and analyzed in a ”comparison map” approach involving 16 subregions. For information extracted from the ocular region around the Iris, two types of features are used. One is an LBP representation of the texture, and the other is based (SIFT) points.
4	Three steps Approach	Shin, Nam et al. 2012	1-D Gabor wavelet for textural information.	The 1st step is a classification method which discriminates the ”left or right eye”. Second, is the separability between intra- and inter-classes is increased by using the 2nd step classification based on the ”color information” of the iris region. Third, ”textural information” of the iris region is used for the 3rd step classification. That is, the 1-D Gabor wavelet filter is applied to the red, green, and gray image channels to afford three sets of iris codes from iris textures.

A conclusion that can be drawn from the best competition results NICE II is that the fusion of multiple information sources. Using more than one type of texture feature extraction on the iris region and fusing the results improves the performance in comparison with any one of the Iris texture features. Other conclusion we reached is that using features extracted from the iris region combined with features extracted from the ocular region is better that use only the features from the iris region. The top-performing algorithm uses two sources of information from the Iris region and two from the ocular region. Because the top-ranked algorithms seem to have relatively distinct technical approaches, it is likely that a fusion of the top algorithms would result in further performance improvement[134].

Tabla 4. *Table 3.* (*Continued*) Eight best-ranked algorithms in NiceII competition.

No.	Method	Author	Feature extraction technique	Description
5	WCPH	Li, Liu et al. 2012	weighted co-occurrence phase histogram.	The method proposes a weighting function that enables a phase angle to make contributions to several adjacent bins; the co-occurrence histogram considers the information of both the phase angle and spatial layout.
6	LBP-BLOB	Marsico, Nappi et al. 2012	Linear Binary Patterns.	Divided the iris image into horizontal (or vertical). For each band, the histogram of LBP values is computed. They use (BLOBs) to extract and code blob features is. They obtain matrix with both positive and negative values, and then binarized by setting all negative values to 0 and all positive values to 1.
7	2D Gabor	Li and Ma 2012	2D Gabor.	The authors performed over a set of candidate 2D Gabor filters to select the particular ones to be used in creating the Iris code.
8	Reverse Biorthogonal Wavelet Transform	Szewczyk, Grabowski et al. 2012	Wavelet transform (rbio 3. 1 V4)	The 512×256 image is cropped to 256×256 to remove influence of eyelashes on Iris pattern and further decrease in computation of the signature encoding and a histogram equalization step is performed. For the 256×256 image, the level-four wavelet decomposition results in 324 coefficients.

4. Challenges in Iris Feature Extraction

Considering that iris recognition is still relatively new (20 years old) there is a need for continued research and tests in the following areas: new challenges, limitations well-known and answer the unknown questions. Changes in iris feature extraction will be tied to the new trends of iris recognition. Under this new generation of iris recognition can be highlighted[37]:

- Video-based non-cooperative iris recognition. iris recognition technology continues to mature, it will gain the ability to acquire an image even without the knowledge of the end user. This will make iris recognition a great way to verify people because it will cause no extra burden for the user. This technology also has great potential for finding people of interest, because a non-cooperative iris recognition system can identify people without the making the person aware they are being identified. This application is particularly valuable for security at airport, borders or any others public places.
- Multiple wavelength based iris recognition. Near infra-red (NIR) images have been dominant in iris identification. A disadvantage of NIR light is that it requires active NIR illumination. Visible wavelength iris recognition could function using environmental illumination. In addition, visible wavelength recognition is important because it can be used with facial recognition for multimodal biometrics. In the future, regular color surveillance camera may have the capability to perform iris recognition. Visible wavelength iris recognition has its own challenges, especially it is challenging for dark color eyes and remote iris recognition. In the future, multiple-wavelength iris recognition may raise

more attention and will be able to work together with multiple-wavelength face recognition for video surveillance.

- Multimodal eye recognition. The iris patterns of dark color eyes could reveal rich and complex patterns only under NIR light, if the NIR iris image are obtained in a long distance, the accuracy of iris recognition will drop dramatically. And if we acquire iris image in visible light, the iris patterns of dark color eyes will be hardly visible under visual light. The sclera, the white and opaque outer protective covering of the eye, can also be used in human identification. The segmentation process of the sclera image, includes image down-sampling, conversion to the HSV color space, estimation of the sclera region, iris and eyelid detection, eyelid and iris boundary refinement, mask creation, and mask. All these issues are challenges to be faced by biometric iris recognition.

In this sense, it is a challenge get a method of feature extraction which is able to handling a set of parameters during this process. This is the case of parameters that depend on environmental factors during the image acquisition. For example problems related to the visible light, off-angle iris, pupil dilation, use of contact lenses and others.

Currently is working on a new multibiometric method integrating face, iris and eye regions, and it is a challenge to design biometric features to be common to these biometrics modalities but which are easily to extract from then and with good properties to identify people.

5. Conclusions

Researches in feature extraction methods for iris recognition have been widely adressed to obtain techniques and algorithms for robust iris recognition over the last few years. However key and still open issue in iris recognition is how best to represent the iris texture information using a compact set of iris texture features. This report has reviewed many approaches regarding Iris Features Extraction Methods from the pioneering in iris recognition, Daugman's 2D Gabor and Wildes's Laplacian of Gaussian, up to algorithms for feature extraction in non-cooperative environment. We have identified two major approaches and new emerging trend: 1) Daugman's method, which is the most important work in the early history of iris biometrics. It is fair to say that iris biometrics as a field has been developed under the concepts of Daugman's approach which become a standard reference model. 2) The Ordinal Measures for iris recognition proposed by[40], not only because this novel method is more effective than existing algorithms, the results obtained from it provide a better explanation of how the best state of the art iris recognition algorithms work effectively. An emerging and challenging area is Non-cooperative iris recognition, that can make iris recognition more friendly and flexible to use, this also we will allow its further use in video surveillance and multi-biometric systems.

References

1. Rashad, M., Shams, M., Nomir, O., El-Awady, R.: Iris recognition based on lbp and combined lvq classifier. International Journal of Computer Science **3**(5) (2011) 67–78
2. Dorairaj, V., Schmid, N.A., Fahmy, G.: Performance evaluation of iris based recognition system implementing pca and ica encoding techniques (2005)
3. Zhang, H., Sun, Z., Tan, T., Wang, J.: Iris image classification based on color information. In: 21st International Conference on Pattern Recognition (ICPR 2012). 3427–3430
4. Ng, R.Y.F., Yong Haur, T., Kai Ming, M.: Dsp-based implementation and optimization of an iris verification algorithm using textural feature. In: Fuzzy Systems and Knowledge Discovery, 2009. FSKD '09. Sixth International Conference on. Volume 5. 374–378

5. H.B.Kekre, Thepade, S.D., Jain, J., Agrawal, N.: Iris recognition using texture features extracted from haarlet pyramid. International Journal of Computer Applications **11**(12) (2010) 1–5
6. Daugman, J.G.: High confidence visual recognition of persons by a test of statistical independence. Pattern Analysis and Machine Intelligence, IEEE Transactions on **15**(11) (1993) 1148–1161
7. Nabti, M., Bouridane, A.: An effective and fast iris recognition system based on a combined multiscale feature extraction technique. Pattern Recognition **41**(3) (2008) 868–879
8. Tan, T., Zhang, X., Sun, Z., Zhang, H.: Noisy iris image matching by using multiple cues. Pattern Recogn. Lett. **33**(8) (2012) 970–977
9. Balas, V., Motoc, I., Barbulescu, A.: Combined haar-hilbert and log-gabor based iris encoders. New Concepts and Applications in Soft Computing (2012) 1–26
10. Santos, G., Hoyle, E.: A fusion approach to unconstrained iris recognition. Pattern Recogn. Lett. **33**(8) (2012) 984–990
11. Kumar, S.D.R., Raja, K.B., Chhootaray, R.K., Pattnaik, S.: Pca based iris recognition using dwt. International Journal of Computer Technology and Applications **2**(4) (2010) 884–893
12. Patil, P.S.: Iris recognition based on gaussian-hermite moments. International Journal on Computer Science and Engineering (IJCSE) **4**(11) (2012) 1794–1803
13. Bertillon, A.: La couleur de liris. Annales de Demographie Internationale **7** (1886) 226–246
14. Flom, L., Safir, A.: Iris recognition system (1987)
15. Rakesh, T., Khogare, M.G.: Survey of biometric recognition system for iris. International Journal of Emerging Technology and Advanced Engineering **2**(6) (2012) 272–276
16. Bowyer, K.W., Hollingsworth, K., Flynn, P.J.: Image understanding for iris biometrics: A survey. Comput. Vis. Image Underst. **110**(2) (2008) 281–307
17. Li, Y.h., Savvides, M. In: Iris Recognition, Overview. Springer US (2009) 810–819
18. Duda, R.O., Hart, P.E., Stork, D.G.: Pattern classification. 2 edn. Wiley (2001)
19. Li, S., Jain, A.: Encyclopedia of Biometrics: I - Z. Springer (2009)
20. Ma, L., Wang, Y., Tan, T.: Iris recognition based on multichannel gabor filtering. In: Proceedings of the International Conference on Asian Conference on Computer Vision. (2002) 279–283
21. Tuceryan, M., Jain, A.K. In: Texture analysis. World Scientific Publishing Co., Inc. (1998) 207–248
22. Hyvärinen, A., Oja, E.: Independent component analysis: algorithms and applications. Neural networks **13**(4) (2000) 411–430
23. Ojala, T., Pietikinen, M., Harwood, D.: A comparative study of texture measures with classification based on featured distributions. Pattern Recognition **29**(1) (1996) 51–59
24. Sun, Z., Tan, T., Qiu, X.: Graph matching iris image blocks with local binary pattern (2006)
25. Tian, Q., Qu, H., Zhang, L., Zong, R.: 8. In: Personal Identity Recognition Approach Based on Iris Pattern. (2011) 314
26. Marsico, M.D., Nappi, M., Riccio, D.: Noisy iris recognition integrated scheme. Pattern Recogn. Lett. **33**(8) (2012) 1006–1011
27. Li, P., Liu, X., Zhao, N.: Weighted co-occurrence phase histogram for iris recognition. Pattern Recognition Letters **33**(8) (2012) 1000–1005
28. Hyvrinen, A.: What is independent component analysis ? (April 2003 Retrieved 2012)
29. Ya-Ping, H., Si-wei, L., En-Yi, C.: An efficient iris recognition system. In: Machine Learning and Cybernetics, 2002. Proceedings. 2002 International Conference on. Volume 1. 450–454 vol.1
30. Chowhan, S.S., Shinde, G.N.: Evaluation of statistical feature encoding techniques on iris images. In: Computer Science and Information Engineering, 2009 WRI World Congress on. Volume 7. 71–75
31. Bouraoui, I., Chitroub, S., Bouridane, A.: Does independent component analysis perform well for iris recognition? Intelligent Data Analysis **16**(3) (2012) 409–426
32. Jong-Gook, K., Youn-Hee, G., Jang-Hee, Y., Kyo-IL, C.: A novel and efficient feature extraction method for iris recognition. ETRI Journal **29** (2007) 399401
33. Rathgeb, C., Uhl, A.: 27. In: Secure Iris Recognition Based on Local Intensity Variations. Volume 6112 of Lecture Notes in Computer Science. Springer Berlin Heidelberg (2010) 266–275
34. Rathgeb, C., Uhl, A., Wild, P.: 3. In: State-of-the-Art in Iris Biometrics. Volume 59 of Advances in Information Security. Springer New York (2013) 21–36
35. Ebrahimzadeh, R., Jampour, M., Yaghoobi, M., Soleimani-Nezhad, A.: Towards a fast method for iris identification with fractal and chaos game theory. International Journal of Pattern Recognition and Artificial Intelligence **26**(4) (2012) 14
36. Wildes, R.P.: Iris recognition: an emerging biometric technology. Proceedings of the IEEE **85**(9) (1997) 1348–1363
37. Nanavati, R.: Biometric data safeguarding technologies analysis and best practices. Technical report, DTIC Document (2011)
38. Lu, C., Lu, Z.: Local feature extraction for iris recognition with automatic scale selection. Image Vision Comput. **26**(7) (2008) 935–940

39. Chou, C.T., Shih, S.W., Chen, W.S., Cheng, V.W., Chen, D.Y.: Non-orthogonal view iris recognition system. Circuits and Systems for Video Technology, IEEE Transactions on **20**(3) (2010) 417–430
40. Sun, Z., Tan, T.: Ordinal measures for iris recognition. Pattern Analysis and Machine Intelligence, IEEE Transactions on **31**(12) (2009) 2211–2226
41. Sun, Z., Tan, T., Wang, Y.: Robust encoding of local ordinal measures: A general framework of iris recognition (2004)
42. Sun, Z., Tan, T., Wang, Y.: Iris recognition based on non-local comparisons (2004)
43. Balas, B.J., Sinha, P.: Dissociated dipoles: Image representation via non-local comparisons (2003)
44. Zhaofeng, H., Zhenan, S., Tieniu, T., Xianchao, Q., Cheng, Z., Wenbo, D.: Boosting ordinal features for accurate and fast iris recognition. In: Computer Vision and Pattern Recognition, 2008. CVPR 2008. IEEE Conference on. 1–8
45. Wang, L., Sun, Z., Tan, T.: Robust regularized feature selection for iris recognition via linear programming (November 11-15, 2012 2012)
46. Ruderman, D.L., Cronin, T.W., Chiao, C.C.: Statistics of cone responses to natural images: Implications for visual coding. Journal of the Optical Society of America A **15** (1998) 2036–2045
47. Gabor, D.: Theory of communication. part 1: The analysis of information. Electrical Engineers - Part III: Radio and Communication Engineering, Journal of the Institution of **93**(26) (1946) 429–441
48. Masek, L.: Recognition of human iris patterns for biometric identification. Technical report (2003)
49. Yu, L., Zhang, D., Wang, K.: The relative distance of key point based iris recognition. Pattern Recogn. **40**(2) (2007) 423–430
50. Pschernig, E.: Cancelable biometrics for iris detection with parameterized wavelets and wavelet packets. PhD thesis (2009)
51. Qiu, X., Sun, Z., Tan, T.: Learning appearance primitives of iris images for ethnic classification. In: Image Processing, 2007. ICIP 2007. IEEE International Conference on. Volume 2. II – 405–II – 408
52. Al-Qunaieer, F.S.: COLOR IRIS RECOGNITION AND MATCHING USING QUATERNION GABOR WAVELETS. PhD thesis (2009)
53. Wang, Q., Zhang, X., Li, M., Dong, X., Zhou, Q., Yin, Y.: Adaboost and multi-orientation 2d gabor-based noisy iris recognition. Pattern Recognition Letters **33**(8) (2012) 978–983
54. Wang, D., Hou, Y., Peng, J.: Partial Differential Equations Methods in Image Processing. Science Press,, Beijing (2008)
55. Field, D.J.: Relations between the statistics of natural images and the response properties of cortical cells. J. Opt. Soc. Am. A **4**(12) (1987) 2379–2394
56. Peng, Y., Li, J., Ye, X., Zhuang, Z., Li, B.: Iris recognition algorithm using modified log-gabor filters. In: Pattern Recognition, 2006. ICPR 2006. 18th International Conference on. Volume 4. 461–464
57. Seif, A., Zewail, R., Saeb, M., Hamdy, N.: Iris identification based on log gabor filtering. In: Circuits and Systems, 2003 IEEE 46th Midwest Symposium on. Volume 1., IEEE 333–336
58. Farouk, R.M., Elhadi, G.F.: Time of matching reduction and improvement of sub-optimal image segmentation for iris recognition. International Journal of Computer Science **8**(3) (2011) 284–294
59. Bastos, C.A.C.M., Tsang Ing, R., Cavalcanti, G.D.C.: Analysis of 2d log-gabor filters to encode iris patterns. In: Tools with Artificial Intelligence (ICTAI), 2010 22nd IEEE International Conference on. Volume 2. 377–378
60. Jeong, D.S., Park, H.A., Park, K.R., Kim, J.: Iris recognition in mobile phone based on adaptive gabor filter (2006)
61. Ma, L., Tan, T., Wang, Y., Zhang, D.: Personal identification based on iris texture analysis. Pattern Analysis and Machine Intelligence, IEEE Transactions on **25**(12) (2003) 1519–1533
62. Li, M., Yunhong, W., Tieniu, T.: Iris recognition using circular symmetric filters. In: Pattern Recognition, 2002. Proceedings. 16th International Conference on. Volume 2. 414–417 vol.2
63. Guan-Chen, P.: A tutorial of wavelet for pattern recognition (17 January, 2013 Retrieved 2013)
64. Burrus, C.S., Gopinath, R.A., Guo, H., Odegard, J.E., Selesnick, I.W.: Introduction to wavelets and wavelet transforms: a primer. Volume 23. Prentice hall Upper Saddle River (1998)
65. Jian-Jiun, D.: Time frequency analysis tutorial gabor feature and its aapplication (Retrieved 2012)
66. Zhu, Y., Tan, T., Wang, Y.: Biometric personal identification based on iris patterns. In: Pattern Recognition, 2000. Proceedings. 15th International Conference on. Volume 2. 801–804 vol.2
67. Ma, L., Tan, T., Wang, Y., Zhang, D.: Efficient iris recognition by characterizing key local variations. Image Processing, IEEE Transactions on **13**(6) (2004) 739–750
68. Xiaofu, H., Pengfei, S.: Extraction of complex wavelet features for iris recognition. In: Pattern Recognition, 2008. ICPR 2008. 19th International Conference on. 1–4
69. Bodade, R.M., Talbar, S.N.: Shift invariant iris feature extraction using rotated complex wavelet and complex wavelet for iris recognition system. In: Advances in Pattern Recognition, 2009. ICAPR '09. Seventh International Conference on. 449–452
70. Tajbakhsh, N., Misaghian, K., Bandari, N.: 39. In: A Region-Based Iris Feature Extraction Method Based on 2D-Wavelet Transform. Volume 5707 of Lecture Notes in Computer Science. Springer Berlin Heidelberg (2009) 301–307
71. Chen, C.H., Chu, C.T.: High performance iris recognition based on 1-d circular feature extraction and pso-pnn classifier. Expert Syst. Appl. **36**(7) (2009) 10351–10356

72. Harjoko, A., Hartati, S., Dwiyasa, H.: A method for iris recognition based on 1d coiflet wavelet. world academy of science, engineering and technology **56**(24) (2009) 126–129
73. Nasare, R.M., Hase, S.G., More, V.: Iris recognition by complex wavelet transform. International Journal of Engineering and Innovative Technology (IJEIT) **1**(4) (2012) 119–123
74. Sachane, M., Jain, V.: Iris feature extraction using wavelet maxima components for biometric identification systems (May 19th 2012)
75. Boles, W.W., Boashash, B.: A human identification technique using images of the iris and wavelet transform. Signal Processing, IEEE Transactions on **46**(4) (1998) 1185–1188
76. de Martin-Roche, D., Sanchez-Avila, C., Sanchez-Reillo, R.: Iris recognition for biometric identification using dyadic wavelet transform zero-crossing. In: Security Technology, 2001 IEEE 35th International Carnahan Conference on, IEEE 272–277
77. Sanchez-Avila, C., Sanchez-Reillo, R.: Two different approaches for iris recognition using gabor filters and multiscale zero-crossing representation. Pattern Recognition **38**(2) (2005) 231–240
78. Hoyle, E., Feitosa, R., Petraglia, A.: Iris recognition using one-dimensional signal analysis (June 17 19 2009)
79. Rampally, D.: Iris recognition based on feature extraction. Technical report, Kasas State University (2010)
80. Kumar, A., Passi, A.: Comparison and combination of iris matchers for reliable personal authentication. Pattern Recogn. **43**(3) (2010) 1016–1026
81. Kwanyong, L., Shinyoung, L., Kwanyong, L., Okhwan, B., Taiyun, K.: Efficient iris recognition through improvement of feature vector and classifier. ETRI Journal **23** (2001) 61–70
82. Daouk, C., El-Esber, L., Kammoun, F., Al Alaoui, M.: Iris recognition. In: IEEE ISSPIT. (2002) 558–562
83. Tze Weng, N., Thien Lang, T., Siak Wang, K.: Iris recognition using rapid haar wavelet decomposition. In: Signal Processing Systems (ICSPS), 2010 2nd International Conference on. Volume 1. V1–820–V1–823
84. Panganiban, A., Linsangan, N., Caluyo, F.: Wavelet-based feature extraction algorithm for an iris recognition system. Journal of Information Processing Systems **7**(3) (2011) 425–434
85. Birgale, L., Kokare, M.: Comparison of color and texture for iris recognition. International Journal of Pattern Recognition and Artificial Intelligence **26**(03) (2012) 1256007
86. Narote, S.P., Narote, A.S., Waghmare, L.M.: Iris based recognition system using wavelet transform. International Journal of Computer Science and Network Security (IJCSNS) **9**(11) (2009) 101–104
87. Laine, A., Fan, J.: Texture classification by wavelet packet signatures. Pattern Analysis and Machine Intelligence, IEEE Transactions on **15**(11) (1993) 1186–1191
88. Turkoglu, I., Arslan, A., Ilkay, E.: An intelligent system for diagnosis of the heart valve diseases with wavelet packet neural networks. Computers in biology and medicine **33**(4) (2003) 319–331
89. Rydgren, E., Thomas, E.A., Amiel, F., Rossant, F., Amara, A.: Iris features extraction using wavelet packets. In: Image Processing, 2004. ICIP '04. 2004 International Conference on. Volume 2. 861–864 Vol.2
90. Gan, J., Liang, Y.: 59. In: Applications of Wavelet Packets Decomposition in Iris Recognition. Volume 3832 of Lecture Notes in Computer Science. Springer Berlin Heidelberg (2005) 443–449
91. Lokhande, S., Bapat, V..N.: Iris recognition for biometric identification using wavelet packet decomposition. International Journal of Engineering Research and Technology (IJERT) **1**(4) (2012) 1–7
92. Lokhande, S., Vishram . N., B.: Wavelet packet based iris texture analysis for person authentication. Signal and Image Processing : An International Journal (SIPIJ) **4**(2) (2013) 91–104
93. Patil, C.M., Patilkulkarani, S.: Iris feature extraction for personal identification using lifting wavelet transform. In: Advances in Computing, Control, and Telecommunication Technologies, 2009. ACT '09. International Conference on. 764–766
94. Zhonghua, L., Bibo, L.: Iris recognition method based on the coefficients of morlet wavelet transform (2010)
95. Khalighi, S., Tirdad, P., Pak, F., Nunes, U.: Shift and rotation invariant iris feature extraction based on non-subsampled contourlet transform and glcm (2012)
96. Ahmed, N., Natarajan, T., Rao, K.R.: Discrete cosine transform. Computers, IEEE Transactions on **C-23**(1) (1974) 90–93
97. Alim, O.A., Sharkas, M.: Iris recognition using discrete wavelet transform and artificial neural networks. In: Circuits and Systems, 2003 IEEE 46th Midwest Symposium. Volume 1. 337–340 Vol. 1
98. Monro, D.M., Rakshit, S., Dexin, Z.: Dct-based iris recognition. Pattern Analysis and Machine Intelligence, IEEE Transactions on **29**(4) (2007) 586–595
99. Dhavale, S.V.: Dwt and dct based robust iris feature extraction and recognition algorithm for biometric personal identification. International Journal of Computer Applications **40**(7) (2012) 33–37 Published by Foundation of Computer Science, New York, USA.
100. Mehrotra, H., Srinivas, B.G., Majhi, B., Gupta, P. In: Indexing iris biometric database using energy histogram of DCT subbands. Springer (2009) 194–204
101. Popescu-Bodorin, N., Balas, V.E.: Comparing haar-hilbert and log-gabor based iris encoders on bath iris image database. In: Soft Computing Applications (SOFA), 2010 4th International Workshop on, IEEE 191–196

102. Anand, K., Tiwari, A., Verma, M., Singh, A.: Iris recognition. VSRD International Journal of Electrical, Electronics and Communication Engineering **2**(10) (2012) 854–858
103. Peng-Fei, Z., De-Sheng, L., Qi, W.: A novel iris recognition method based on feature fusion. In: Machine Learning and Cybernetics, 2004. Proceedings of 2004 International Conference on. Volume 6. 3661–3665 vol.6
104. Daugman, J.G.: Complete discrete 2-d gabor transforms by neural networks for image analysis and compression. Acoustics, Speech and Signal Processing, IEEE Transactions on **36**(7) (1988) 1169–1179
105. Daugman, J.: How iris recognition works. Circuits and Systems for Video Technology, IEEE Transactions on **14**(1) (2004) 21–30
106. Salih, Q.A., Dhandapani, V.: Iris recognition based on multi-channel feature extraction using gabor filters (2006)
107. Gulmire, K., Ganorkar, S.: Iris recognition using gabor wavelet. International Journal of Engineering Research and Technology (IJERT) **1**(5) (2012)
108. Belcher, C., Du, Y.: Region-based sift approach to iris recognition. Optics and Lasers in Engineering **47**(1) (2009) 139–147
109. Du, Y., Belcher, C., Zhou, Z.: Scale invariant gabor descriptor-based noncooperative iris recognition. EURASIP J. Adv. Signal Process **2010** (2010) 1–13
110. Lowe, D.G.: Distinctive image features from scale-invariant keypoints. Int. J. Comput. Vision **60**(2) (2004) 91–110
111. Park, H.A., Park, K.R.: Iris recognition based on score level fusion by using svm. Pattern Recogn. Lett. **28**(15) (2007) 2019–2028
112. Shin, K.Y., Nam, G.P., Jeong, D.S., Cho, D.H., Kang, B.J., Park, K.R., Kim, J.: New iris recognition method for noisy iris images. Pattern Recognition Letters **33**(8) (2012) 991–999
113. Zhang, M., Sun, Z., Tan, T.: Deformed iris recognition using bandpass geometric features and lowpass ordinal features. In: Proceedings of the 6th IAPR International Conference on Biometrics, (ICB2013)
114. da Cunha, A.L., Jianping, Z., Do, M.N.: The nonsubsampled contourlet transform: Theory, design, and applications. Image Processing, IEEE Transactions on **15**(10) (2006) 3089–3101
115. Li, X., Wang, L., Sun, Z., Tan, T.: A feature-level solution to off-angle iris recognition. In: Proceedings of the 6th IAPR International Conference on Biometrics, (ICB2013)
116. Santos, G., Proenca, H.: Iris recognition: Analyzing the distribution of the iriscodes concordant bits. In: Image and Signal Processing (CISP), 2010 3rd International Congress on. Volume 4. 1873–1877
117. Gawande, U., Zaveri, M.A., Kapur, A.: Improving iris recognition accuracy by score based fusion method. International Journal of Advancements in Technology (IJoAT) **1**(1) (2010) 1–12
118. Boles, W.W.: A security system based on human iris identification using wavelet transform. In: Knowledge-Based Intelligent Electronic Systems, 1997. KES '97. Proceedings., 1997 First International Conference on. Volume 2. 533–541 vol.2
119. Feddaoui, N., Mahersia, H., Hamrouni, K.: Improving iris recognition performance using quality measures. Advanced Biometric technologies (2010) 242–264
120. Feddaoui, N., Mahersia, H., Hamrouni, K.: Iris recognition method based on gabor filters and uniform local binary patterns. International Journal of Image and Graphics **12**(02) (2012)
121. Kumar, D., Raja, K., Nuthan, N., Sindhuja, B., Supriya, P., Chhotaray, R., Pattnaik, S.: Iris recognition based on dwt and pca. Computational Intelligence and Communication Networks (CICN), 2011 International Conference on (2011) 489–493
122. Proenca, H., Santos, G.: Fusing color and shape descriptors in the recognition of degraded iris images acquired at visible wavelengths. Comput. Vis. Image Underst. **116**(2) (2012) 167–178
123. Monaco, M.K.: Color space analysis for iris recognition. PhD thesis (2007)
124. Kong, A.W.K., Zhang, D., Kamel, M.: 16. In: An Introduction to the IrisCode Theory. Springer (2013) 321–336
125. Vatsa, M., Singh, R., Gupta, P.: Comparison of iris recognition algorithms. In: Intelligent Sensing and Information Processing, 2004. Proceedings of International Conference on. 354–358
126. Daugman, J.: High confidence recognition of persons by iris patterns. In: IEEE 35th International Carnahan Conference on Security Technology. 254–263
127. Tisse, C.L., Martin, L., Torres, L., Robert, M.: Iris recognition system for person identification (2002)
128. Thornton, J., Savvides, M., Kumar, B.: An evaluation of iris pattern representations. In: Biometrics: Theory, Applications, and Systems, 2007. BTAS 2007. First IEEE International Conference on, IEEE 1–6
129. Sheela, S.V., Vijaya, P.A.: Iris recognition based on wavelets. International Journal of Computer Applications **26**(11) (2011) 47–54
130. Du, Y.: Using 2d log-gabor spatial filters for iris recognition. In: SPIE 6202: Biometric Technology for Human Identification III. Volume 6202. 62020F–62020F–8 10.1117/12.663834.
131. Krichen, E., Mellakh, M.A., Garcia-Salicetti, S., Dorizzi, B.: Iris identification using wavelet packets. In: Pattern Recognition, 2004. ICPR 2004. Proceedings of the 17th International Conference on. Volume 4. 335–338 Vol.4
132. Liu, C., Xie, M.: Iris recognition based on dlda (2006)
133. Thornton, J., Savvides, M., Kumar, B.V.K.V.: Robust iris recognition using advanced correlation techniques (2005)
134. Bowyer, K.W.: The results of the nice.ii iris biometrics competition. Pattern Recogn. Lett. **33**(8) (2012) 965–969

RT_060, febrero 2014
Aprobado por el Consejo Científico CENATAV

Editor: Lic. Lucía González Bayona
Diseño de Portada: Di. Alejandro Pérez Abraham
RNPS No. 2142
ISSN 2072-6287
Indicaciones para los Autores:
Seguir la plantilla que aparece en www.cenatav.co.cu
C E N A T A V
7ma. A No. 21406 e/214 y 216, Rpto. Siboney, Playa;
La Habana. Cuba. C.P. 12200
Impreso en Cuba